

Booklet JDN 2021  
20-22 september 2021

# Monday 20th of september

Time	Title - Speaker	Room	Page
13h30	Welcome Ceremony	Main Room	
13h45	The contribution of neutron scattering to the low-temperature water conundrum J. Teixeira	Main Room	6
14h30	Study of the excitations for the understanding of the matter properties K. Beauvois	Room A	7
14h30	Multiscale nature of water confinement in clay porous media E. Ferrage	Room B	8
15h10	Break	Mingling Floor	
15h40	In-situ neutron diffraction during reversible deuterium loading of Mn-substituted TiFe alloys E. Dematteis	Room A	9
15h40	Nanoconfining H <sub>2</sub> - manipulation of the phase diagram and consequences of reduced freedom L. Terry	Room B	10
16h00	QENS study of the diffusivity of hydrogen in MoS <sub>2</sub> V. Kuznetsov	Room A	11
16h00	Clay nanotubes: order-disorder transition and water confinement A. D'Angelo	Room B	12
16h20	Experimental probe of the non-bonded interaction potential in endofullerenes: <sup>3</sup> He@C <sub>60</sub> study M. Aouane	Room A	13
16h20	Revealing molecular level structure property relationships of Nafion composite proton exchange membranes K. Smith	Room B	14
16h40	Importance of lattice softness and phonon anharmonicity for the optoelectronic properties of 3D, 2D and 0D halide perovskites J. Even	Room A	15
16h40	Linking structural and mechanical properties within hydrogels based on ionene polyelectrolytes and clay nanoplatelets C. Hotton	Room B	16
17h00 17h15 17h30 17h45	News from neutrons centers : ILL — J. Jestin ESS — A. Hiess 2FDN — M. Plazanet LLB — G. Chaboussant	Main Room	

## Tuesday 21th of september

Time	Title - Speaker	Room	Page
13h30	Fishing for polymer and nanoparticles in nanocomposites using SANS, SAXS, and simulations J. Oberdisse	Main Room	18
14h00	PhD Award presentation	Main Room	
14h45	Break	Mingling Floor	
15h10	Continuum of magnetic excitations and short-range order in the 2D quantum triangular magnet ErMgGaO <sub>4</sub> S. Bhattacharya	Room A	19
15h10	Dynamics of apolipoprotein B-100 assessed by incoherent neutron scattering A. Cisse	Room B	20
15h30	Spin Dynamics and Unconventional Coulomb Phase in Nd <sub>2</sub> Zr <sub>2</sub> O <sub>7</sub> S. Petit	Room A	21
15h30	Assessing the <i>in situ</i> protein corona structure L. Marichal	Room B	22
15h50	Magnetic properties of single-crystalline clinoatacamite, Cu <sub>2</sub> Cl(OH) <sub>3</sub> , a distorted kagomé compound L. Heinze	Room A	23
15h50	Effects of stabilizers on the protein-like dynamical transition of PNIPAM: a neutron scattering study B. Rosi	Room B	24
16h10	Structural and magnetic disorder in defect spin ice Ho <sub>2</sub> Ti <sub>1.5</sub> Sc <sub>0.5</sub> O <sub>6.75</sub> T.S. Northam	Room A	25
16h10	Diffusive dynamics in crowded solutions containing two types of proteins L. Colin	Room B	26
16h30	Neutron Diffraction Study of NaMgD <sub>3</sub> at High Pressure J.A. Nunez	Room A	27
16h30	Picosecond dynamics of polymorphs of lysozyme aggregates with different levels of cytotoxicity T. Matsuo	Room B	28
16h50	Implementation of in-situ neutron characterization techniques for the characterization of metal additive manufacturing B. Ozcan	Room A	29
16h50	Monitoring food structure in plant protein gels during digestion: from rheometry to small-angle neutron scattering M. Napieraj	Room B	30
17h10	Exploring the D–Hf phase diagram using in-situ neutron diffraction M. Dottor	Room A	31
17h10	Insertion and activation of functional bacteriorhodopsin in a floating bilayer T. Mukhina / G. Fragneto	Room B	32
17h30	Présentation ENSA et AG SFN	Main Room	

## Wednesday 22th of september

Time	Title - Speaker	Room	Page
13h30	Loop currents in quantum matter P. Bourges	Main Room	34
14h30	In situ study of energy materials by neutron diffraction L. Laversenne	Room A	35
14h30	Following surfactant assemblies in foams A. Salonen	Room B	36
15h10	Break	Mingling Floor	37
15h40	Unforeseen combination of magnetism and superconductivity in the pressurized BaFe <sub>2</sub> Se <sub>3</sub> spin ladder W. Zheng	Room A	38
15h40	Revealing the nature of $\pi$ ···H – O weak interaction via neutron total scattering C. Di Mino	Room B	39
16h00	Advance magnetocaloric materials for adiabatic demagnetization: Spin dynamics of the quantum dipolar magnet Yb <sub>3</sub> Ga <sub>5</sub> O <sub>12</sub> E. Riordan	Room A	40
16h00	(De)stabilization of non-ionic foam with ions J. Lamolinaire	Room B	41
16h20	Surface magnons and crystalline electric field shifts at the nanoscale in superantiferromagnetic NdCu <sub>2</sub> E.M. Jefremovas	Room A	42
16h20	SANS studies of polyelectrolytes in organic media A. Gulati	Room B	43
16h40	Field-space anisotropy in the magnetic phase diagrams and multipolar excitations of Ce <sub>1-x</sub> La <sub>x</sub> B <sub>6</sub> measured in a rotating magnetic field D.S. Inosov	Room A	44
16h40	Surface pressure-induced interdiffused structure evidenced by neutron reflectometry in cellulose acetate/polybutadiene Langmuir films A. El Haitami	Room B	45
17h00	Instrumentation session - On the use of statistical choppers to increase the performances of diffraction instruments on HiCANS — F. Ott	Main Room	46-49
17h20	- LLB CRG Inelastic instruments at ILL: from IN6 to Sharp, then Sharp+ — J.-M. Zanotti		
17h40	- Autonomous Experiments in Inelastic Neutron Scattering — M. Boehm		
18h00	- NeXT-Grenoble, the Neutron and X-rat Tomograph at ILL — A. Tengattini		

Abstracts for  
Monday 20th of september

# The contribution of neutron scattering to the low-temperature water conundrum

J. Teixeira<sup>1</sup>

<sup>1</sup> *Université Paris-Saclay, CNRS, CEA, Laboratoire Léon Brillouin, 91191 Gif-sur-Yvette, France.*

Water is ubiquitous yet remains a liquid that is not well understood. The so-called anomalous thermodynamic properties, e.g. the density maximum, remain poorly explained at the atomic level. The complexity results from the directional bonds that form between neighboring molecules. However, the effective potentials replace the spherical molecule and the anisotropic potential by electric charges. They must always find a compromise between an excess of structure and an insufficient description of the anomalies. This is especially true at low temperature, in the metastable domain of supercooled water.

The presentation discusses the relevance of recently proposed mixture models, which do not comply with small angle scattering measurements. We then present models based on the dynamics of hydrogen bonding. Quasi-elastic neutron scattering experiments identify two characteristic times and geometric considerations allow them to relate. The supercooling limit (around 228 K), often associated with critical behaviors, then becomes a dynamic transition analogous to those observed in polymers, where one goes from the non-Arrhenius anomalous behavior of molecular dynamics to the Arrhenius dynamics of hydrogen bonds alone at very low temperature.

# Study of the excitations for the understanding of the matter properties

K. Beauvois<sup>ab</sup>, V. Simonet<sup>c</sup>, S. Petit<sup>d</sup>, J. Robert<sup>c</sup>, F. Bourdarot<sup>b</sup>, M. Gospodinov<sup>e</sup>, A. A. Mukhin<sup>f</sup>,  
R. Ballou<sup>c</sup>, V. Skumryev<sup>g</sup> and E. Ressouche<sup>b</sup>

<sup>a</sup> Institut Laue Langevin, Grenoble, France

<sup>b</sup> CEA, IRIG/MEM-MDN, Grenoble, France

<sup>c</sup> Institut Néel-CNRS, Grenoble, France <sup>d</sup> CEA-CNRS, LLB Saclay, France

<sup>e</sup> Institute of Solid State Physics, Bulgarian Academy of Sciences, Bulgaria <sup>f</sup> Russian Academy of Sciences, Russia

<sup>g</sup> Universitat Autònoma de Barcelona, Spain

<sup>h</sup> Buffalo, NY, USA and Johannes Kepler University, Linz, Austria

<sup>i</sup> Centro Atómico Bariloche, San Carlos de Bariloche, Argentina

The study of the excitations is essential in condensed matter physics. For example, the electron-phonon coupling is at the origin of the superconductivity for the superconductors of BCS type. Another example is the superfluidity that is a natural consequence of the dynamics represented by a sharp phonon-roton collective mode in the canonical correlated Bose fluid, liquid 4He. A direct observation of the excitations is possible thanks to neutron scattering techniques. To illustrate it, I will present the study of the excitations in the frustrated Cairo pentagonal antiferromagnet Bi<sub>2</sub>Fe<sub>4</sub>O<sub>9</sub>, which presents various facets of unconventional magnetism.

The research field of magnetic frustration is dominated by triangle-based lattices but exotic phenomena can also be observed in pentagonal networks, as the well-known Cairo lattice. We demonstrate it here with the prototypical Bi<sub>2</sub>Fe<sub>4</sub>O<sub>9</sub> material, where a peculiar noncollinear magnetic order is stabilized, resulting from the geometric frustration and a complex connectivity with three- and four-fold connected Fe1 and Fe2 sites [1]. Firstly, we show the rich magnetic excitation spectrum, obtained by inelastic neutron scattering, where both collective excitations and local modes are present [2]. Those are related to local precession of pairs of spins due to the complex geometry of the lattice. From a comparison with spin wave calculations, we determined the antiferromagnetic superexchange interactions whose competition is confirmed to be at the origin of the spin arrangement. This analysis additionally unveils a hierarchy in the interactions, leading to a paramagnetic state constituted of strongly coupled dimers separated by much less correlated spins, a highly correlated fluid remaining the physics of helium. This produces two types of response to an applied magnetic field associated with the two nonequivalent Fe sites, as observed in the magnetization distributions obtained using polarized neutrons.

# Multiscale nature of water confinement in clay porous media

***E. Ferrage***<sup>1</sup>, E. Tertre<sup>1</sup>, F. Hubert<sup>1</sup>, B. Dazas<sup>1</sup>, E. Paineau<sup>2</sup>, M. Jiménez-Ruiz<sup>3</sup>, P. Porion<sup>4</sup>, A. Delville<sup>4</sup> and L.J. Michot<sup>5</sup>

<sup>1</sup>*IC2MP-Hydrasa, UMR 7285 CNRS, Université de Poitiers, 86022 Poitiers, France*

<sup>2</sup>*Laboratoire de Physique des Solides, CNRS-Université Paris Saclay, Orsay, France*

<sup>3</sup>*Institut Laue-Langevin, Grenoble, France*

<sup>4</sup>*ICMN, UMR 7374 CNRS, Université d'Orléans, 45071 Orléans, France*

<sup>5</sup>*PHENIX, UMR 82324 CNRS, Université Pierre & Marie Curie, 72522 Paris, France*

Clay minerals are lamellar phyllosilicates representing one of the fundamental constituents of numerous terrestrial and marine environments on Earth, including soils and sedimentary rocks. The submicrometric particle sizes of clay particles most often account for a major proportion of the specific surface area of the whole material, leading to strong interactions with surrounding water.

The understanding of water status and diffusional properties in compacted clay-based porous media has a considerable importance in the fields of nuclear waste storage in deep geological formations or for the design of innovative materials with fluid barrier efficiency. Because of their lamellar shape, clay particles most often display a preferred orientation, leading to anisotropy in the morphology of the pore network and having significant impact on the transfer properties of water and other species. For this reason upscaling approaches for water diffusion in clay-based materials are most often based on a the consideration of a dual porosity medium with (i) the bidimensional diffusion in interlayer space of the particles and (ii) the diffusion in the interparticle porosity driven by the mutual arrangements of these flat particles.

At the particle scale, the combination of experimental neutron-based diffraction/scattering techniques and molecular simulations can be used to unravel the details in the organizational and dynamical properties of the fluid confined in the interlayers of swelling clay minerals. In addition, such a collation procedure provides key quantitative information about the validity of the semi-empirical atomic interaction parameters used in theoretical simulations. At higher length scales, in addition to the development of imaging techniques, recent progress has been made in the development of three-dimensional numerical representative porous media. These computed granular systems can account for the heterogeneity in size, morphology, and orientation of clay particles and can be validated using a large set of diffraction or scattering techniques. This presentation will focus on how neutron-based techniques can be used for the validation of numerical models allowing a detailed description of the multiscale nature of water confinement and dynamics in clay porous media.

# In-situ neutron diffraction during reversible deuterium loading of Mn-substituted TiFe alloys

**E. M. Dematteis**<sup>1,2</sup>, J. Barale<sup>1</sup>, G. Capurso<sup>3</sup>, S. Deledda<sup>4</sup>, F. Cuevas<sup>2</sup>, M. Latroche<sup>2</sup> and M. Baricco<sup>1</sup>

<sup>1</sup> Department of Chemistry, Inter-departmental Center Nanostructured Interfaces and Surfaces (NIS), and INSTM, University of Turin, Via Pietro Giuria 7, 10125 Torino, Italy

<sup>2</sup> Univ Paris Est Creteil, CNRS, ICMPE, UMR 7182, 2 rue Henri Dunant, 94320 Thiais, France

<sup>3</sup> Institute of Materials Research, Helmholtz-Zentrum Geesthacht, Max-Planck-Str. 1, 21502 Geesthacht, Germany

<sup>4</sup> Institute for Energy Technology, Kjeller, NO-2027, Norway

Hydrogen is an efficient energy carrier that can be produced from renewable sources and stored in alloys in solid-state for long period enabling the transition towards CO<sub>2</sub>-free energy. Binary TiFe intermetallic compound can store 1.86 wt.% H<sub>2</sub>. [1] TiFe<sub>0.90</sub> (*i.e.* Ti substitution at the Fe site in TiFe) exhibits a milder activation process for the first hydrogenation, and Ti(Fe,Mn)<sub>0.90</sub> substituted alloys can lead fine tuning of equilibrium pressure as a function of the final application. [2] In this study, the crystal structure of TiFe<sub>(0.90-x)</sub>Mn<sub>x</sub> alloys ( $x = 0, 0.05$  and  $0.10$ ) and their deuterides have been determined by in-situ neutron diffraction while recording Pressure-Composition Isotherm curves at room temperature. The alloy compositions have been selected within a promising composition range for an integrated, renewable, large-scale stationary hydrogen storage tank within the framework of the HyCARE European project ([www.hycare-project.eu](http://www.hycare-project.eu)). The investigation aims at analysing the influence of Mn and Ti substitutions at the Fe site for TiFe-type alloys on structural properties during reversible deuterium loading, still unsolved and unexplored. Alloys are synthesized by induction furnace and annealed at 1000 °C. After activation, samples have been transferred into a custom made stainless-steel cell used for in-situ neutron diffraction experiments during deuterium loading at ILL and ISIS neutron facilities. [3,4]. The evolution of diffraction line positions and intensities was followed as a function of hydrogen pressure to determine domains of existence for the three detected phases ( $\alpha$ : D-solution in pristine alloy,  $\beta$ : mono-deuteride and  $\gamma$ : di-deuteride) as displayed in **Figure 1** for sample TiFe<sub>0.85</sub>Mn<sub>0.05</sub>. This structural study enables remarkable understanding on hydrogen storage, basic structural knowledge, and support to the industrial application of TiFe-type alloys for integrated hydrogen tank in energy storage systems.

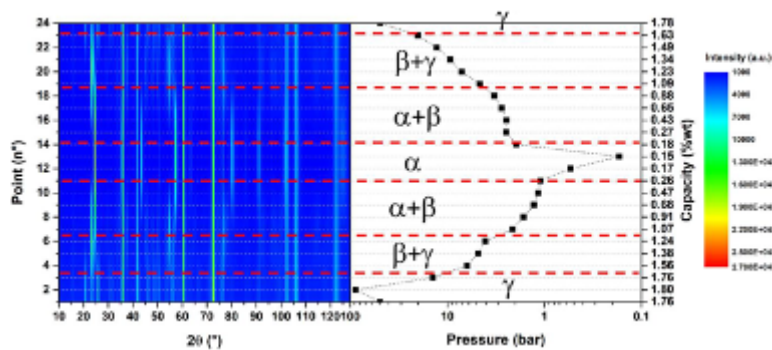


**Fig.1 – In -situ neutron diffraction analysis of TiFe<sub>0.85</sub>Mn<sub>0.05</sub> during a full absorption-desorption cycle.**

[1] Bannenberg, L.J.; Heere, M.; Benzidi, H.; Montero, J.; Dematteis, E.M.; et al. Metal (boro-) hydrides for high energy density storage and relevant emerging technologies. *Int. J. Hydrogen Energy* 2020, 45, 33687–33730, doi:10.1016/j.ijhydene.2020.08.119.

[2] Dematteis, E.M.; Berti, N.; Cuevas, F.; Latroche, M.; Baricco, M. Substitutional effects in TiFe for hydrogen storage: a comprehensive review. *Mater. Adv.* 2021, 2, 2524–2560, doi:10.1039/D1MA00101A.

[3] Cuevas, F.; Deledda, S.; Dematteis, E.M.; Hauback, B.C.; Latroche, M.; Laversenne, L.; Zhang, J. In-situ neutron diffraction during reversible deuterium loading in under-stoichiometric and Mn-substituted Ti(Fe,Mn)0.9 alloys. *Inst. Laue-Langevin* 2020, doi:10.5291/ILL-DATA.5-22-771.

[4] Dematteis, E.M.; Hauback, B.C.; da Silva Gonzalez, I.; Deledda, S.; Cuevas, F.; Latroche, M.; Capurso, G.; Barale, J. In-situ neutron diffraction during reversible deuterium loading in under-stoichiometric and Mn,Cu-substituted Ti(Fe,Mn,Cu)0.9 alloys. *STFC ISIS Neutron Muon Source* 2019, doi:10.5286/ISIS.E.RB1920559-1.

# Nanoconfining H<sub>2</sub> – manipulation of the phase diagram and consequences of reduced freedom

**Lui. R. Terry**<sup>1</sup>, Stephane Rols<sup>2</sup>, Mi Tian<sup>3</sup>, Simon Bending<sup>4</sup>, Valeska Ting<sup>1\*</sup>

<sup>1</sup> *Department of Mechanical Engineering, University of Bristol, UK*

<sup>2</sup> *Institute Laue Langevin, Grenoble, France*

<sup>3</sup> *College of Engineering, Mathematics and physical sciences, University of Exeter, UK*

<sup>4</sup> *Department of Physics, University of Bath, UK*

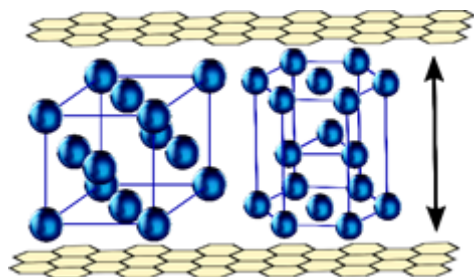
As an energy-dense, potentially sustainable energy vector, as well as a potential room-temperature superconductor, condensed phases of hydrogen will play a major role in the future of our energy systems. Nevertheless, a fundamental limitation to the study and application of dense, solid phases of molecular hydrogen (H<sub>2</sub>) is that they generally only form at exceedingly low temperatures or extremely high pressures.

Confinement of H<sub>2</sub> in nanoscale pores of carbon nanomaterials, however, has enabled formation of solid-like H<sub>2</sub> at atmospheric pressure at temperatures above the critical point [1-3]. To understand the potential of nanoconfinement for manipulation of the hydrogen phase diagram, examination of the solids that form inside nanoscale pores and why is needed.

Using a powerful combination of variable temperature and variable-pressure neutron diffraction and inelastic neutron scattering (INS), here we study both the structure and rotational dynamics of H<sub>2</sub> confined in microporous and mesoporous activated carbons.

Revealing the crystal structures of H<sub>2</sub> confined in activated carbon for the first time and uncovering significant manipulation of the phase diagram of H<sub>2</sub>. We clarify the observed effects by changes to the molecular arrangement and quantum rotations of individual nuclear spin isomers of H<sub>2</sub> in the pore network.

The results of this study indicate how the thermal stability of solid phases of H<sub>2</sub> could be increased with further material design and how other interesting non-equilibrium condensed phases of hydrogen could be achieved.



[1] Ting, V. P. et al. Direct Evidence for Solid-like Hydrogen in a Nanoporous Carbon Hydrogen Storage Material at Supercritical Temperatures. *ACS Nano* 9, 8249–8254 (2015).

[2] Gallego, N. C., He, L., Saha, D., Contescu, C. I. & Melnichenko, Y. B. Hydrogen Confinement in Carbon Nanopores: Extreme Densification at Ambient Temperature. *J. Am. Chem. Soc.* 133, 13794–13797 (2011).

[3] He, L. et al. Investigation of morphology and hydrogen adsorption capacity of disordered carbons. *Carbon* N. Y. 80, 82–90 (2014)

## **QENS study of the diffusivity of hydrogen in MoS<sub>2</sub>**

**V. Kuznetsov**<sup>1,2</sup>, W. Lohstroh<sup>3</sup>, D. Rogalla<sup>4</sup>, H.-W. Becker<sup>4</sup>, T. Strunskus<sup>5</sup>, A. Nefedov<sup>6</sup>, E. Kovacevic<sup>7</sup>, F. Traeger<sup>2</sup> and P. Fouquet<sup>1</sup>

<sup>1</sup>*Institut Laue-Langevin, Grenoble, France*

<sup>2</sup>*Westfälische Hochschule, Recklinghausen, Germany*

<sup>3</sup>*TU München, FRM II, Garching, Germany*

<sup>4</sup>*RUBION, Ruhr-Universität Bochum, Bochum, Germany*

<sup>5</sup>*Universität Kiel, Kiel, Germany*

<sup>6</sup>*Karlsruher Institut für Technologie (KIT), Eggenstein-Leopoldshafen, Germany*

<sup>7</sup>*GREMI, Orléans, France*

With an increase in renewable energy production, the problem of energy storage becomes more and more significant. One of the most promising ideas is storage in form of hydrogen gas, which involves the production of hydrogen by electrolysis and later reconversion of hydrogen in fuel cells. It is of paramount importance for these processes to be carried out most efficiently with the most readily accessible materials. Therefore, there have been intense studies in the search for catalyst materials for the hydrogen and oxygen evolution reactions, in order to replace the expensive platinum, which is widely used today.

Molybdenum disulphide, MoS<sub>2</sub>, has shown promising behavior as a catalyst in the hydrogen evolution reaction (HER), which is completely in line with its known activity for hydrogenation reactions. In this presentation we will show the results of our study of the diffusion of hydrogen adsorbed inside layered MoS<sub>2</sub> crystals, for which we used quasielastic neutron scattering, neutron spin-echo spectroscopy, nuclear reaction analysis, and X-ray photoelectron spectroscopy [1]. The neutron time-of-flight and neutron spin-echo measurements demonstrate fast diffusion of hydrogen molecules parallel to the basal planes of the two dimensional crystal planes. At room temperature and above, this intra-layer diffusion is of a similar speed to the surface diffusion that has been observed in earlier studies for hydrogen atoms on Pt surfaces. A much slower hydrogen diffusion was observed perpendicular to the basal planes using nuclear reaction analysis.

[1] Vitalii Kuznetsov, Wiebke Lohstroh, Detlef Rogalla, Hans-Werner Becker, Thomas Strunskus, Alexei Nefedov, Eva Kovacevic, Franziska Traeger and Peter Fouquet, *Physical Chemistry Chemical Physics* 23 (2021) 7961 – 7973.

# Clay nanotubes: order-disorder transition and water confinement

*A. D'Angelo*<sup>1,2</sup>, E. Paineau<sup>1</sup>, P. Launois<sup>1</sup> and S. Rols<sup>2</sup>

<sup>1</sup> *Laboratoire de Physique des Solides, CNRS-Université Paris Saclay, Orsay, France*

<sup>2</sup> *Institut Laue-Langevin, Grenoble, France*

Imogolite is a nanotubular clay material, with stoichiometry  $(\text{OH})_3\text{Al}_2\text{O}_3\text{Si}(\text{OH})$ . Thanks to its small inner diameter ( $\sim 1.5$  nm), it is a model system for studying the dynamics of nanoconfined water, which can exhibit radically different properties in comparison to those of bulk water. An imogolite nanotube is hydrophilic because its inner wall is covered with hydroxyl groups.

Recent investigations on an imogolite-like nanotube with inner diameter  $\sim 2.8$  nm, where silicon was replaced by germanium, showed that  $\text{H}_2\text{O}$  molecules in contact with the surface are stabilized by the formation of three H-bonds with the nanotube wall, resulting in a single water wetting-layer strongly bound and solid-like up to 300K [1].

Our study focuses on aluminosilicate imogolite nanotubes and on the process of water adsorption inside their internal cavity. As it seems that the flexibility and mobility of the inner hydroxyls are the main responsible for water structuring, we first focused on the study of a tube in dry conditions, and afterwards on water confinement. The results presented here were obtained by elastic and inelastic neutron scattering experiments, combined with Molecular Dynamics (MD) simulations using a pre-existent parametrization for the interaction potential of the imogolite [2]. In the dry state, an original transition is evidenced from a state where inner OH bonds have the same orientation (as shown in Fig. 1) to a disordered state. The simulated density of states of the absorbed water will be compared to its equivalent in the case of aluminogermanate imogolite nanotube and will also be confronted to experimental data obtained using inelastic neutron scattering for aluminosilicate imogolite [3, DAngelo-ILLexp\_report]. We will thus be able to highlight the singularities of nanoconfined water in imogolite nanotubes.

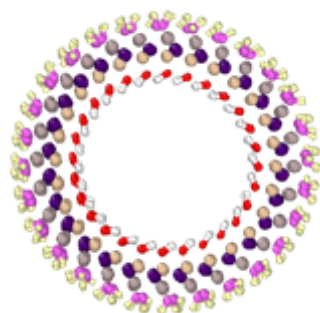


**Figure 1. Top view of an imogolite nanotube in its low temperature state, having the inner hydroxyls (inner oxygen in red; inner hydrogen in white) aligned in the same direction.**

[1] G. Monet et al., *Nanoscale Advances*, 2 (2020) 1869-1877

[2] L. Scalfi et al., *Langmuir*, 34 (2018) 6748–6756

[3] Le Caër et al., *Nanoscale Advances*, 3 (2021), 789-799

# Experimental probe of the non-bonded interaction potential in endofullerenes: $^3\text{He}@C_{60}$ study

**M. Aouane**<sup>a\*</sup>, S. Rols<sup>a</sup>, R.J. Whitby<sup>b</sup> and M.H. Levitt<sup>b</sup>

1. Institut Laue-Langevin, BP 156, 38042 Grenoble, France

b. School of Chemistry, University of Southampton, Southampton, SO17 1BJ, UK

\* email: aouanem@ill.fr

Endofullerenes are supramolecular complexes consisting of a small (endohedral) atom/molecule enclosed by a fullerene ( $C_{60}$ ) cage<sup>[1,2]</sup>. Endofullerenes offer experimentalists with the molecular realisation of the ideal particle-in-a-box model, which enables one to directly observe translational (atomic) quantisation. The resulting energy diagram is sensitive to the intermolecular interaction potential.

The aim of this study is firstly to observe transitions arising purely from atomic translational quantization due to confinement of a helium atom inside an almost spherical cage. Secondly, one aims at obtaining a detailed characterisation of the translational energy levels in an enlarged energy scale in order to derive experimentally the confining potential for the  $\text{He}@C_{60}$  complex. In this talk, it will show that from neutron spectroscopy data, one can obtain information about the potential function  $V(r)$  representing the non-bonded interaction between the He atom and the  $C_{60}$  cage. Mainly showing it to be a superposition of  $r^2$ ,  $r^4$ , and  $r^6$  terms, which in turn can be tested against different theoretical models. Experiments of this kind provide high-quality experimental benchmarks for quantum chemistry calculations of non-bonded intermolecular and interatomic interactions.

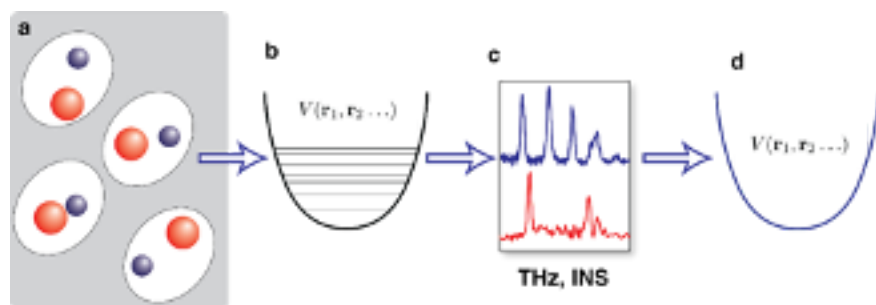


**Figure 1:** Analysis of the spectroscopic data allows determination of the potential energy function of the atom trapped in the  $C_{60}$

[1] Levitt MH. 2013 Spectroscopy of light-molecule endofullerenes. Phil Trans R Soc A 371:20120429.

[2] K. S. K. Goh, M. Jimenez-Ruiz, M. R. Johnson, S. Rols, J. Ollivier, M. S. Denning, S. Mamone, M.H.Levitt, X. Lei, Y. Li, N. J. Turro, Y. Murata and A. J. Horsewill, Phys. Chem. Chem. Phys., 2014, 16, 21330-21339.

# Revealing Molecular Level Structure Property Relationships of Nafion Composite Proton Exchange Membranes

**K. Smith**<sup>1</sup>, F. Foglia<sup>2</sup>, S. Lyonnard<sup>3</sup>, Victoria García Sakai<sup>4</sup>, Quentin Berrod<sup>3</sup>, Gérard Gebel<sup>5</sup>, T. S. Miller<sup>1\*</sup>, P. F. McMillan<sup>2\*</sup> and D. J. L. Brett<sup>1\*</sup>

<sup>1</sup> *Electrochemical Innovation Lab, Department of Chemical Engineering, UCL, London WC1E 7JE, United Kingdom*

<sup>2</sup> *Department of Chemistry, Christopher Ingold Laboratory, UCL, 20 Gordon St., London WC1H 0AJ, United Kingdom*

<sup>3</sup> *Univ. Grenoble Alpes, CNRS, CEA, IRIG-SyMMES, 38000 Grenoble, France.*

<sup>4</sup> *ISIS Neutron and Muon Source, Rutherford Appleton Laboratory, Harwell Science and Innovation Campus, Chilton OX11 0QX, United Kingdom.*

<sup>5</sup> *Univ. Grenoble Alpes, CEA LITEN, 38000 Grenoble, France.*

Sustainable energy generation and storage devices are critical to mitigate the continued impacts of climate change. Proton exchange membranes (PEM) are essential components of energy storage and conversion devices, such as fuel cells, electrolyzers and redox flow batteries. They are essential in conducting protons between electrodes, whilst preventing the transport of fuel molecules and electrolyte ions, such as H<sub>2</sub>, CH<sub>3</sub>OH and VO<sup>2+</sup>. Despite half a century of polymer development, perfluorinated sulfonic acid (PFSA) membranes, such as Nafion, remain the industry standard. It exhibits high proton conductivity as a result of a complex phase separated morphology between hydrophobic tetrafluoroethylene backbone and hydrophilic sulfonic acid terminated side chains that provide proton hopping sites.

Hydration of the polymer has a large impact on performance due to the formation of contiguous hydrated ionic domains where protons are conducted via Grotthuss and vehicular diffusion in the hydrated phase. This requirement for high hydration and thus sub 100 °C operation in a humidified setup is the main drawback of PFSA polymers. Incorporating nanoparticles into the PFSA matrix has led to PEMs with enhanced performance and provides a simple route to overcome the issues of water management, low temperature operation and fuel crossover. Two-dimensional materials have been intensely investigated due to their large surface area maximizing polymer – particle interaction within the matrix.<sup>[1,2]</sup> However, the way in which these nanoparticles tune the multifarious microstructure of the composite membrane and interact with the PFSA chains leading to alternative, enhanced, proton conduction mechanisms is poorly understood and requires fundamental investigation.

We have recently revealed selective diffusion of H<sub>2</sub>O through the C<sub>12</sub>N<sub>12</sub> ring voids of the basal planes of crystalline polytriazine imide (PTI) structured gCN layers, which make it an attractive additive candidate.<sup>[3]</sup> We have successfully incorporated varying quantities of PTI and graphene oxide (GO) separately into the Nafion matrix with enhanced proton conductivity. The aim of this work was to utilise neutron scattering techniques to understand how both these particles, of different chemical functionality and size, lead to favourable molecular level structural and dynamical changes. Neutron reflectivity (NR) and small angle neutron scattering (SANS) investigation at varying membrane hydrations and isotope exchange has revealed structural organisation for film thicknesses of different orders of magnitude and provides insight to the mechanism by which GO enhances water uptake. Quasi-elastic neutron scattering (QENS) was then used to probe slow (0.9 μeV) and fast (25.4 μeV) proton populations at low and high hydrations and correlated their geometry with information from structural investigation. Relating these results with device level testing has allowed greater understanding of the fundamental factors which drive the change in material properties. The overall understanding of structural and functional properties in this array of composites provides a base understanding to design future high performance membranes for energy conversion and storage devices.

[1] Z. Chen, Y. Peng, F. Liu, Z. Le, J. Zhu, G. Shen, D. Zhang, M. Wen, S. Xiao, C. P. Liu, Y. Lu and H. Li, *Nano Lett.*, 15 (2015) 6802–6808.

[2] P. Velayutham and A. K. Sahu, *J. Phys. Chem. C*, 122 (2018) 21735–21744.

[3] F. Foglia, A. J. Clancy, J. Berry-Gair, K. Lisowska, M. C. Wilding, T. M. Suter, T. S. Miller, K. Smith, F. Demmel, M. Appel, V. García Sakai, A. Sella, C. A. Howard, M. Tyagi, F. Corà and P. F. McMillan *Sci. Adv.*, 6 (2020) eabb6011

# Importance of lattice softness and phonon anharmonicity for the optoelectronic properties of 3D, 2D and 0D halide perovskites

**J. Even**<sup>1</sup>, A.C. Ferreira<sup>1,2</sup>, S. Paofai<sup>3</sup>, A. Létoublon<sup>1</sup>, J. Ollivier<sup>4</sup>, S. Raymond<sup>5</sup>, S. Clément<sup>6</sup>, R. Violla<sup>6</sup>, B. Hehlen<sup>6</sup>, B. Rufflé<sup>6</sup>, S. Cordier<sup>3</sup>, C. Katan<sup>2</sup> and P. Bourges<sup>2</sup>

<sup>1</sup> Univ Rennes, INSA Rennes, CNRS, Institut FOTON-UMR 6082, 35000 Rennes, France.

<sup>2</sup> Université Paris-Saclay, CNRS, CEA, Laboratoire Léon Brillouin, 91191 Gif-sur-Yvette, France.

<sup>3</sup> Univ Rennes, ENSCR, INSA Rennes, CNRS, ISCR-UMR 6226, 35000 Rennes, France.

<sup>4</sup> Institut Laue Langevin, 71 avenue des martyrs, 38000 Grenoble, France.

<sup>5</sup> Univ. Grenoble Alpes, CEA, IRIG, MEM, MDN, 38000 Grenoble, France.

<sup>6</sup> Laboratoire Charles Coulomb, UMR 5221 CNRS-Université de Montpellier, 34095 Montpellier, France.

The joint iFOTON-ISCR perovskite CNRS team in Rennes and LLB-Saclay have performed over the last five years, systematic studies of hybrid halide perovskite 3D materials, using inelastic neutron scattering and triple axis spectrometers located at LLB and ILL. These investigations have focused on the low frequency part of the vibrational density of states, revealing the exceptional softness of this new class of semiconductors dedicated to optoelectronics and the strong anharmonicity of the phonons in the crystal lattice [1-3].

The aim of the presentation will be to emphasize the importance of these findings for ongoing fundamental studies and device characterizations, as well as open questions in the field. 3D halide perovskite bulk discovered in 2009 as photovoltaic materials, are now leading both the field of thin film photovoltaics since 2015 and the film of quantum dot solar cells since 2017, coming close to classical crystalline semiconductors and being attractive for low-cost tandem solar cells [4]. It was further demonstrated in 2016 that 2D layered perovskites improve the stability of operating devices under light soaking [5]. Halide perovskites exhibit in addition a number of structural instabilities [6], detrimental for applications. In that context, it is well-known that neutron spectrometry is helpful to decipher the underlying mechanisms [7]. The softness of the lattice is also expected to play a role for carrier localization in 3D [8] and 2D [9] solar cell during device operation and for carrier trapping in monochromatic [10] or white light [11] emitters. State of the art carrier mobility models based on microscopic descriptions of the electron-phonon interaction [12] are in fair agreement with our findings [1-3], but a proper description of the phonon anharmonicity is still missing [13]. More, delayed intraband relaxation of charged carriers interesting for hot carrier solar cell applications at high temperature [14] are attributed to still poorly understood phonon bottleneck effects [15]. Conversely, for single photon [16] or entangled photon quantum dot sources [17], the absence of one-phonon relaxation to the dark exciton state appears to be at the origin of photon bunching and antibunching at low temperature [18].

[1] A. Létoublon, S. Paofai, B. Rufflé, P. Bourges, B. Hehlen, T. Michel, C. Ecolivet, O. Durand, S. Cordier, C. Katan, J. Even, *J. Phys. Chem. Lett.*, 7 (2016) 3776.

[2] A. Ferreira, A. Létoublon, S. Paofai, S. Raymond, C. Ecolivet, B. Rufflé, S. Cordier, C. Katan, M. Saidaminov, A. Zhumekenov, O. Bakr, J. Even, P. Bourges, *Phys. Rev. Lett.* 121 (2018) 085502. [3] A. Ferreira, S. Paofai, A. Létoublon, J. Ollivier, S. Raymond, B. Hehlen, B. Rufflé, S. Cordier, C. Katan, J. Even, P. Bourges, *Comm. Phys.* 3 (2020) 48. [4] NREL chart for certified solar cell efficiencies (<https://www.nrel.gov/pv/cell-efficiency.html>). [5] H. Tsai, W. Nie, J.-C. Blancon, C. C. Stoumpos, R. Asadpour, B. Harutyunyan, A. Neukirch, R. Verduzco, J. Crochet, S. Tretiak, L. Pedesseau, J. Even, M. Alam, G. Gupta, J. Lou, P. Ajayan, M. Bedzyk, M. Kanatzidis, A. Mohite, *Nature* 536 (2016), 312. [6] J. Even, M. Carignano, and C. Katan, *Nanoscale*, 8 (2016) 6222. [7] P. Bourges, M. H. Lemée-Cailleau, P. Launois, C. Ecolivet, H. Cailleau, F. Moussa, and A. Mierzejewski, *Phys. Rev. B* 54, (1996) 15002. [8] H. Tsai, R. Asadpour, J.-C. Blancon, C. C. Stoumpos, O. Durand, J. Strzalka, B. Chen, R. Verduzco, P. Ajayan, S. Tretiak, J. Even, M. Alam, M. Kanatzidis, W. Nie, A. Mohite, *Science* 360 (2018) 67. [9] J.-C. Blancon, H. Tsai, W. Nie, C. Stoumpos, L. Pedesseau, C. Katan, M. Kepenekian, C. Soe, K. Appavoo, M. Sfeir, S. Tretiak, P. Ajayan, M. Kanatzidis, J. Even, J. Crochet, A. Mohite *Science* 355 (2017) 1288. [10] X. Gong, O. Voznyy, A. Jain, W. Liu, R. Sabatini, Z. Piontkowski, G. Walters, G. Bappi, S. Nokhrin, O. Bushuyev, M. Yuan, R. Comin, D. McCamant, S. Kelley, E. Sargent, *Nature Mat.* 17 (2018) 550. [11] L. Mao, Y. Wu, C. Stoumpos, B. Traore, C. Katan, J. Even, M. Wasielewski, M. Kanatzidis, *J. Am. Chem. Soc.* 139 (2017) 11956 [12] M. Schlipf, S. Poncé, F. Giustino, *Phys. Rev. Lett.* (2018) [13] C. Katan, A. Mohite, J. Even, *Nature Mat.* 17 (2018) 377. [14] H. Fang, S. Adjoktse, S. Shao, J. Even, M. Loi, *Nature Comm.* 9 (2018) 243. [15] Y. Yang, D. Ostrowski, R. France, Kai Zhu, J. Lagemaat, J. Luther, M. Beard, *Nature. Phot.* 10 (2016) 53. [16] M. Fu, P. Tamarat, J.-B. Trebbia, M. Bodnarchuk, M. Kovalenko, J. Even, B. Lounis, *Nature Comm.* 9 (2018) 3318. [17] P. Tamarat, L. Hou, J.-B. Trebbia, A. k Swarnkar, L. Biadala, Y. Louyer, M. Bodnarchuk, M. Kovalenko, J. Even, B. Lounis, *Nature Comm.* 9 (2020) 6001. [18] P. Tamarat, M. Bodnarchuk, J.-B. Trebbia, R. Erni, M. Kovalenko, J. Even, B. Lounis, *Nature Mat.* 18 (2019) 717.

# Linking structural and mechanical properties within hydrogels based on ionene polyelectrolytes and clay nanoplatelets.

**C. Hotton**<sup>1</sup>, J. Sirieix-Plénet<sup>1</sup>, G. Ducouret<sup>2</sup>, T. Bizien<sup>3</sup>, A. Chennevière<sup>4</sup>, L. Porcar<sup>5</sup>, L. Michot<sup>1</sup> and N. Malikova<sup>1</sup>

<sup>1</sup> *Laboratoire PHENIX, Sorbonne Université, CNRS, Paris, France.*

<sup>2</sup> *Laboratoire SIMM, CNRS, ESPCI Paris, PSL Research University, Paris, France.*

<sup>3</sup> *Synchrotron SOLEIL, l'Orme des merisiers, Saint-Aubin - BP 48 91192 Gif-sur-Yvette, France.*

<sup>4</sup> *Laboratoire Léon Brillouin, UMR12 CEA-CNRS-Université Paris-Saclay Gif-sur-Yvette, France.*

<sup>5</sup> *Large Scale Structures, Institut Laue Langevin, Grenoble, France.*

Hydrogels are at the forefront of scientific attention especially in the biomedical field thanks to their high-water content, their mechanical and swelling properties [1]. Association of hydrogel and clay nanoparticles as additives has a great potential in the design of materials that exhibit additional enhanced mechanical, swelling or barrier properties [2]. The functional properties of these materials are intimately linked to their structural organisation.

We investigate the organisation of clay nanoplatelets within a hydrogel based on modified ionenes [3], cationic polyelectrolytes forming physically crosslinked hydrogels induced by hydrogen bonding and  $\pi$ - $\pi$  stacking. Combination of small angle X-ray and neutron scattering (SAXS, SANS) reveals the structure of the polyelectrolyte network as well as the organisation of the clay additives [4]. The clay-free hydrogel network features a characteristic mesh-size between 20 to 30 nm, depending on the polyelectrolyte concentration. Clay nanoplatelets inside the hydrogel organise in a regular face-to-face (stacking) manner, with a large repeat distance, following rather closely the hydrogel mesh-size. This suggests that the nanoplatelets "decorate" the underlying polyelectrolyte network. Further, the clay-compensating counterions ( $\text{Na}^+$ ,  $\text{Ca}^{2+}$  or  $\text{La}^{3+}$ ) and the clay type (montmorillonite, beidellite) both have a significant influence on nanoplatelet organisation. The degree of nanoplatelet ordering in the hydrogel is very sensitive to the negative charge location on the clay platelet (different for each clay type). Increased nanoplatelet ordering leads to an improvement of the elastic properties of the hydrogel. On the contrary, the presence of dense clay aggregates (tactoids), induced by multi-valent clay counterions, destroys the nanoplatelet "decoration" of the hydrogel network and a reduction of elastic modulus of the hydrogel is observed.

In the long-term, rheo-SAXS will be used to shed light on whether the anisotropy of clay nanoparticles could yield an anisotropic mechanical response of the hydrogel [5].

[1] Y. S. Zhang and A. Khademhosseini, *Science*, 356(6337) (2017) 3627.

[2] L. Z. Zhao, C. H. Zhou, J. Wang et al, *Soft Matter*, 11 (2015) 9229

[3] L. Z.Y. Misawa, N. Koumura et al, *Macromolecules*, 41 (2008) 8841-8846.

[4] C. Hotton et al. (in submission)

[5] A. M. Philippe, C. Baravian, V. Bezuglyy et al, *Langmuir*, 2917 (2013) 5315-5324.

Abstracts for  
Tuesday 21th of september

# Fishing for polymer and nanoparticles in nanocomposites using SANS, SAXS, and simulations

*J. Oberdisse*<sup>1</sup> and A.C Genix<sup>1</sup>

<sup>1</sup> *Laboratoire Charles Coulomb(L2C), Université de Montpellier, CNRS, F-34095 Montpellier, France*

Rubber-based nanocomposites prepared by solid-phase mixing with precipitated silica nanoparticles are typically strongly aggregated systems with different levels of spatial organization, as highlighted by our group in the past [1]. The strategy that we developed these past years was to investigate such systems based on the study of simplified industrial samples with ingredients limited to a strict minimum. The analysis of small-angle X-ray scattering data can then be performed on the scale of a micrometric simulation box. Tens of thousands of “model” nanoparticles are embedded in the matrix, and their dispersion strongly affects both the mechanical properties of the material, and the scattered intensity. A statistical method based on a reverse Monte Carlo solution of this many-parameter scattering problem will be presented, showing that some key features like percolation can be described [2].

Another key feature of rubber nanocomposites refers to the influence of the filler surfaces on the polymer structure and dynamics, and some recent progress will be discussed [3]. In particular, we have studied blends of short and long chains, where one chain type is deuterated, by small-angle neutron scattering. Different degrees of spatial segregation could be identified recently, including a peculiar, “fish-shaped” interfacial gradient characterized also by reverse Monte Carlo simulations, this time of the interface.

[1] Guilhem P. Baeza, Anne-Caroline Genix, C. Degrandcourt, Laurent Petitjean, Jérémie Gummel, Marc Couty, Julian Oberdisse, *Macromolecules* 2013, 46, 317–329 (cover article)

[2] Musino D, Genix A-C, Chauveau E, Bizien T, Oberdisse J, *Nanoscale* 2020, 12:3907.

[3] A.C. Genix, V. Bocharova, B. Carroll, P. Dieudonné-George, M. Sztucki, R. Schweins, A. P. Sokolov, and Julian Oberdisse, *ACS Applied Materials and Interfaces*, 2021, in press

# Continuum of magnetic excitations and short-range order in the 2D quantum triangular magnet $\text{ErMgGaO}_4$

S. Bhattacharya<sup>1</sup>, Z. Cronkwright<sup>2</sup>, Q. Berrod<sup>3</sup>, J.-M. Zanotti<sup>3</sup>, B. Gaulin<sup>2</sup>, E. Kermarrec<sup>1</sup>

<sup>1</sup> *Laboratoire de Physique des Solides, Université Paris-Saclay, Orsay, France*

<sup>2</sup> *Department of Physics and Astronomy, McMaster University, Hamilton, Ontario, L8S 4M1, Canada*

<sup>3</sup> *Institut Laue-Langevin - 71 avenue des Martyrs CS 20156, 38042 GRENOBLE Cedex 9 - France*

The 2D antiferromagnetic triangular lattice provides an archetypical geometry for frustrated magnetism, such that near-neighbor interactions cannot be simultaneously satisfied for all neighboring magnetic ions occupying the lattice. In case of an anisotropic triangular lattice, a simple  $J_1$ - $J_2$  model is known to display an extensive quantum spin liquid region, what has motivated several experimental studies. Recently, significant efforts have been made to investigate  $\text{YbMgGaO}_4$ , a  $S_{\text{eff}} = 1/2$  2D-triangular antiferromagnet, that shows an absence of any clear magnetic order according to  $\mu\text{SR}$  measurements [1] simultaneously with a continuum of magnetic excitations observed in inelastic neutron scattering [2]. While these evidence qualify  $\text{YbMgGaO}_4$  as a promising quantum spin liquid candidate, the presence of chemical disorder (Mg/Ga substitution) cast some doubts on the real origin of the absence of magnetic order [3].

Here, we investigate the sister compound  $\text{ErMgGaO}_4$ , where the rare-earth ion has been replaced by  $\text{Er}^{3+}$ , in order to disentangle the effect of the different contributing factors such as anisotropy and disorder, and to explore the phase diagram. As compared to previous work [5][6], a significant improvement of the sample purity has been achieved. We performed magnetisation measurements and inelastic time-of-flight neutron scattering on the IN6-SHARP spectrometer. Our neutron spectroscopy measurements reveal a dual response in the inelastic channel made of a continuum of excitations extending up to  $\sim 1$  meV and a broad dispersive excitation. Below  $T^* < 6\text{K}$ , we observe the build-up of an elastic signal characteristic of 2D, short-range, magnetic correlations.

Our results bring some valuable insights to understand the low- $T$  physics of the quantum spin liquid candidate  $\text{YbMgGaO}_4$  and further help to test the theoretical phase diagram relevant to the  $S_{\text{eff}}=1/2$  2D triangular antiferromagnet model.

[1] Li *et al.*, Phys. Rev. Lett. **117**, 097201 (2016)

[2] Paddison *et al.*, Nature Phys **13**, 117–122 (2017)

[3] Li *et al.*, Phys. Rev. Lett. **118**, 107202 (2017)

[4] Zhu *et al.*, Phys. Rev. Lett. **119**, 157201 (2017)

[5] Cevallos *et al.*, Solid State Comm. **276** 5-8 (2018)

[6] Cai *et al.*, Phys. Rev. B. **101**, 094432, (2020)

# Dynamics of apolipoprotein B-100 assessed by incoherent neutron scattering

A. Cisse<sup>1,2\*</sup>, K. Kormüller<sup>3\*</sup>, A.-L. Schachner-Nedherer<sup>3</sup>, G. Leitinger<sup>4</sup>, R. Prassl<sup>3</sup> and J. Peters<sup>1,2</sup>

<sup>1</sup> Univ. Grenoble-Alpes, CNRS, LiPhy, Grenoble, France

<sup>2</sup> Institut Laue-Langevin (ILL), Grenoble, France

<sup>3</sup> Gottfried Schatz Research Center for Cell Signaling, Metabolism and Aging, Biophysics Division, Medical University of Graz, Graz, Austria

<sup>4</sup> Gottfried Schatz Research Center for Cell Signaling, Metabolism and Aging, Division of Cell Biology, Histology and Embryology, Medical University of Graz, Graz, Austria

Protein dynamics is pivotal to fulfill protein function. Apolipoprotein B-100 is a giant monomeric protein with a fascinating dynamical history: it mediates the conversion from very low density lipoprotein (VLDL, ~50 nm) to low density lipoprotein (LDL, 22 nm). As a key-player in the cholesterol transport system, the protein is intimately linked to the development of atherosclerosis and cardiovascular diseases. However, if studies about whole LDL were conducted using various techniques, including neutron scattering [1,2], no study focused on the sole apo B-100 protein so far. The isolation procedure, which remains quite challenging, relies on the use of a non-ionic detergent; Nonidet P-40 (NP40). Despite huge and repeated efforts, the detergent remains linked to the protein, and cannot be removed from the solution. As a consequence, the NP40 contribution needs to be taken into account. In that way, besides apo B-100 + NP40 sample, as a D<sub>2</sub>O-hydrated powder, pure NP40 detergent needed to be measured.

We first employed elastic incoherent neutron scattering (EINS) experiments to assess the local motions in isolated apo B-100, and compare it to those in VLDL and LDL complexes, published in [2]. EINS scans were carried out from 20 to 315 K at the backscattering spectrometer IN13 (energy resolution of 8  $\mu\text{eV}$ ) at the Institut Laue Langevin (ILL), Grenoble, France. The mean-square displacements (MSD) as a measure of flexibility, and the mean force constant  $\langle k \rangle$  to quantify structural resilience [3] were calculated.

On the other hand, quasi-elastic incoherent neutron scattering (QENS) at 300 K were performed at two different instruments of ILL ; the time-of-flight spectrometer IN5 (energy resolution of 10  $\mu\text{eV}$ ), and the backscattering spectrometer IN16b in BATS mode (4  $\mu\text{eV}$  energy resolution) and classical mode (0.9  $\mu\text{eV}$  resolution). This covering of three different time windows, from respectively 100 ps to around 1 ns, enabled to delimit apo B-100 dynamics (see the figure below). In order to separate contributions of the protein and detergent, a custom model for the Lorentzian areas was used, which accounts for the experimental ratio between apo B-100 and NP40. This new approach, in combination with a classical analysis of the Lorentzian linewidths [4], permitted to retrieve precise parameters of the slow dynamics of apo B-100, and to estimate its interaction with NP40 detergent.

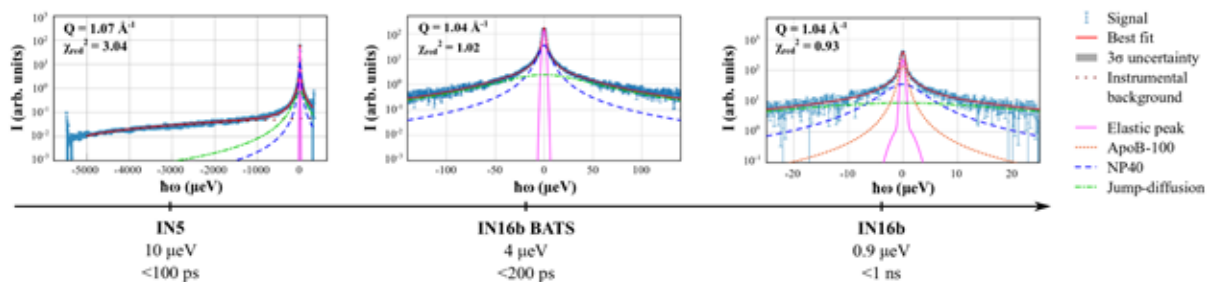


**Figure 1. QENS scans of apo B-100 + NP40 sample for each instrument at one Q-value**

¶

[1] M. Golub, B. Lehofer, N. Martinez, J. Ollivier, J. Kohlbrecher, R. Prassl and J. Peters, Scientific Reports, 7 (2017) 1-11.

[2] C. Mikl, J. Peters, M. Trapp, K. Kormueller, W. J. Schneider, and R. Prassl, Journal of the American Chemical Society, 133 (2011) 13213-13215.

[3] G. Zaccai, Science, 288 (2000) 1604-1607.

[4] F. Volino and A. J. Dianoux, Molecular Physics, 41 (1980) 271-279.

# Spin Dynamics and Unconventional Coulomb Phase in $\text{Nd}_2\text{Zr}_2\text{O}_7$

**M. Léger**<sup>1,2</sup>, E. Lhotel<sup>2</sup>, M. Ciomaga Hatnean<sup>3</sup>, J. Ollivier<sup>4</sup>, A. R. Wildes<sup>4</sup>, S. Raymond<sup>5</sup>, E. Ressouche<sup>5</sup>,  
G. Balakrishnan<sup>3</sup> and S. Petit<sup>1</sup>

<sup>1</sup> LLB, Université Paris-Saclay, CNRS, CEA, CE-Saclay, F-91191 Gif-sur-Yvette, France

<sup>2</sup> Institut Néel, CNRS and Université Grenoble Alpes, 38000 Grenoble, France

<sup>3</sup> Department of Physics, University of Warwick, Coventry CV4 7AL, United Kingdom

<sup>4</sup> Institut Laue Langevin, F-38042 Grenoble, France

<sup>5</sup> Université Grenoble Alpes, CEA, IRIG, MEM, MDN, 38000 Grenoble, France

Geometrical frustration is well known to be one of the key ingredients leading to unconventional states of matter, especially in magnetism. Among them, spin ice and more generally Coulomb phases have attracted significant interest. These can be considered as an original state of matter formed by disordered degenerate configurations where local degrees of freedom remain strongly constrained at the local scale by an organizing principle. In the case of spin ice, these degrees of freedom are Ising spins, sitting on the sites of a pyrochlore lattice formed of corner sharing tetrahedra and aligned along the  $\langle 111 \rangle$  axes, which connect the corners of the tetrahedra to their center. The organizing principle, the “ice rule,” states that each tetrahedron should have two spins pointing in and two out, in close analogy with the hydrogen position in water ice. Importantly, the idea that this local constraint can be considered as the conservation law of an “emergent” magnetic flux ( $\text{div } \mathbf{B} = 0$ ) was quickly imposed. Quantum fluctuations can cause this flux to change with time, giving rise to an emergent electric field, and eventually to an emergent quantum electromagnetism [1]. Despite much work, however, experimental evidence for this enigmatic physics remains elusive. Indeed, the conditions for the realization of this so-called quantum spin ice state are drastic: transverse terms have to be sizable in the Hamiltonian to enable fluctuations out of the local Ising axes, but should remain small enough to prevent the stabilization of classical phases, called Higgs phases, characterized by ordered components perpendicular to these axes.

In the recent years, we have studied the Nd based pyrochlore  $\text{Nd}_2\text{Zr}_2\text{O}_7$  pyrochlore, which offers the opportunity to approach this issue. Despite a positive Curie temperature, indicating the existence of *ferromagnetic* interactions, a partial “all-in–all-out” (AIAO) *antiferromagnetic* ordering is observed below  $T_N \approx 300$  mK. Furthermore, the spin wave excitation spectrum is quite original, taking the form of a flat mode [2].

Our recent studies suggest however that just above  $T_N$  (and below 1 K), this compound hosts a correlated state, which could be a remarkable novel example of the Coulomb phase. This phase is described by a “two-in–two-out” rule as in spin ice, but built on a degree of freedom different from the conventional  $\langle 111 \rangle$  Ising one [3].

Furthermore, to check the robustness of this peculiar state, we have studied the role of defects on the ground state and the excitations, using two types of substitutions: titanium instead of zirconium, to directly affect the magnetic interactions, and lanthanum instead of neodymium to reduce the number of magnetic atoms. We show that defects have a low impact on the crystal electric field scheme (inelastic neutron scattering 2T @LLB and Panther@ILL). We have established the (H,T) phase diagram of these doped compounds by measuring the magnetization and the magnetic structure (D23 @ILL, G41 @LLB), showing that the AIAO phase is reinforced by doping. Surprisingly, the excitations are still well defined in spite of disorder (IN5@ILL) and the flat mode is preserved, with the same characteristic gap energy [4].

[1] M. J. P. Gingras and P. A. McClarty, Rep. Prog. Phys. 77, 056501 (2014).

[2] E. Lhotel and al, PRL 115, 197202 (2015), S. Petit and al, Nature Physics 12, 746 (2016)

[3] M. Léger et al to appear in PRL (2021)

[4] M. Léger et al to appear in PRB (2021)

## Assessing the in situ protein corona structure

**Laurent Marichal**<sup>1</sup>, Fabrice Cousin<sup>2</sup>, Gaël Giraudon--Colas<sup>1</sup>, Serge Pin<sup>1</sup>, and Jean Philippe Renault<sup>1</sup>

<sup>1</sup> NIMBE, CEA Saclay, CNRS, Université Paris-Saclay, Gif-sur-Yvette, France

<sup>2</sup> Laboratoire Léon-Brillouin, CEA Saclay, CNRS, Université Paris-Saclay, Gif-sur-Yvette, France

As soon as nanoparticles are placed in a biological medium, dynamic interactions happen between their surfaces and neighbouring biomolecules. Proteins are particularly prone to interactions and can form the so-called protein corona around these particles. This gives a biological identity to nanoparticles that will condition their biodistribution and potential toxicity.

We thoroughly studied the interactions happening between model proteins (myoglobin and hemoglobin) and nanoparticles (silica). We combined a series of physico-chemical techniques such as oxygenation studies, isothermal titration calorimetry, circular dichroism, and small-angle neutron scattering (SANS). First, we found out that hemoglobin have a stronger affinity to silica surface compared to myoglobin, partly because of its larger size [1]. Secondly, adsorbed and free hemoglobin have different oxygenation properties, especially in terms of oxygen affinity (increase of oxygen affinity for adsorbed hemoglobin) [2]. The structure of adsorbed proteins was then assessed by circular dichroism and SANS. Very subtle secondary and tertiary structure changes could be found while the quaternary structure was totally preserved. This indicates that even without altering their structure, proteins adsorbed on nanoparticles can have their function drastically altered.

Finally, SANS studies allowed us to probe the complex structures of the protein corona (Fig.1) [2]. Myoglobin and hemoglobin form a monolayer of proteins around nanoparticle. We could also determine that, in every system studied, protein/nanoparticle interactions lead to a reaction-limited aggregation process. Besides, it was found that even incomplete coronas were organized by short-distance repulsive interactions between adsorbed proteins. For standard proteins such as the ones studied here the term “protein corona” is particularly well-suited even though, this is not a universal phenomenon since very large proteins tend to form open lattices when interacting with nanoparticles [1].

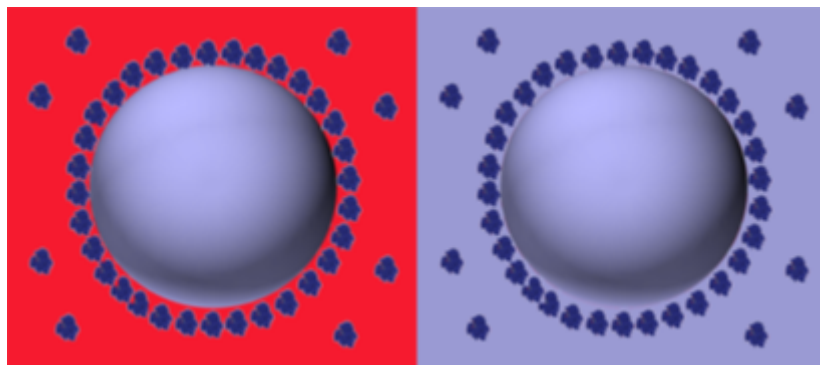


**Figure 1. Schematic representation of the protein/nanoparticle system studied by small-angle neutron scattering. Solutions can be in H<sub>2</sub>O (left) or D<sub>2</sub>O (right) in order to contrast match the nanoparticles to the solvent.**

[1] Marichal L., Degrouard J., Gatin A., Raffray N., Aude J-C, Boulard Y., Combet S., Cousin F., Hourdez A., Mary J., Renault J.-P., and Pin S. *Langmuir*. 36 (2020) 8218-8230.

[2] Marichal L., Giraudon--Colas G., Cousin F., Thill A., Boulard Y., Aude J-C, Labarre J., Pin S., and Renault J.-P. *Langmuir*. 35 (2019) 10831-1083.

# Magnetic properties of single-crystalline clinoatacamite, $\text{Cu}_2\text{Cl}(\text{OH})_3$ , a distorted kagomé compound

L. Heinze<sup>1</sup>, H. O. Jeschke<sup>2</sup>, M. Reehuis<sup>3</sup>, J. Willwater<sup>1</sup>, J. L. Winter<sup>1</sup>, B. Ouladdiaf<sup>4</sup>, K. Beauvois<sup>4</sup>, F. Yokaichiya<sup>3</sup>, J.-U.

Hoffmann<sup>3</sup>, D. Menzel<sup>1</sup>, R. Feyherherm<sup>3</sup>, A. U. B. Wolter<sup>5</sup>, K. C. Rule<sup>6</sup>, and S. Sullow<sup>1</sup>

<sup>1</sup> *Institut für Physik der Kondensierten Materie, TU Braunschweig, 38106 Braunschweig, Germany*

<sup>2</sup> *Research Institute for Interdisciplinary Science, Okayama University, Okayama, Japan*

<sup>3</sup> *Helmholtz-Zentrum Berlin für Materialien und Energie GmbH, 14109 Berlin, Germany*

<sup>4</sup> *Institut Laue-Langevin, 38042 Grenoble Cedex 9, France*

<sup>5</sup> *Leibniz-Institut für Festkörper- und Werkstoffforschung IFW Dresden, 01069 Dresden, Germany*

<sup>6</sup> *Australian Nuclear Science and Technology Organisation, Lucas Heights, NSW 2234, Australia*

Through the search for an experimental realization of a quantum spin liquid state, the atacamite family of copper minerals has come into focus during the last two decades. Especially with the discovery of its member compound herbertsmithite,  $\text{ZnCu}_3\text{Cl}_2(\text{OH})_6$ , as the first promising candidate of an  $S = 1/2$  antiferromagnetic kagomé system, this material family has been investigated intensively and various unusual magnetic properties have been reported. As a member of the Zn paratacamite family,  $\text{Zn}_x\text{Cu}_{4-x}\text{Cl}_2(\text{OH})_6$ , herbertsmithite resides at  $x = 1$ , whereas the end-member compound  $\text{Cu}_2\text{Cl}(\text{OH})_3$  with  $x = 0$  is the natural mineral clinoatacamite.

Clinoatacamite crystallizes in a monoclinic structure with the space group  $P2_1/n$  [1,2]. In the past, studies on polycrystals have shown that this material undergoes magnetic transitions at 18.1 K and 6.4 K [3,4] and the magnetic properties were subsequently studied by various experimental techniques [5–9]. In a neutron diffraction study on deuterated clinoatacamite powder, magnetic reflections with a propagation vector  $\mathbf{q} = \mathbf{0}$  were observed below 6.5 K [6]. No magnetic reflections were observed above this temperature. A zero-field  $\mu\text{SR}$  study revealed a complex temperature evolution of the magnetic state [4], which, in combination with the neutron diffraction measurements, left an incomplete picture of clinoatacamite.

Recently, we have carried out bandstructure calculations for clinoatacamite. By means of DFT and GGA+ $U$  we show that its magnetic coupling scheme can be understood as anisotropic antiferromagnetic kagomé layers with weak ferromagnetic interlayer coupling. From this starting point, we have investigated the magnetic properties of single-crystalline clinoatacamite. We have carried out thermodynamic measurements revealing that the lower magnetic phase transition is in fact a double transition at 6.2 K / 6.4 K and that the temperature region between 6.2 K and 18 K hosts a complex in-field behaviour with various magnetic phases/regimes.

We further study the magnetic phases of clinoatacamite by means of single-crystal neutron diffraction. In zero magnetic field, we have determined the  $\mathbf{q} = \mathbf{0}$  magnetic structure at 2 K and have measured the field and temperature dependence of selected magnetic and nuclear reflections.

[1] J. D. Grice, J. T. Szymanski, and J. L. Jambor, *Can. Mineral.* **34**, 73 (1996).

[2] T. Malcherek and J. Schlüter, *Acta Cryst. B* **65**, 334 (2009).

[3] X. G. Zheng, T. Kawae, Y. Kashitani, C. S. Li, N. Tateiwa, K. Takeda, H. Yamada, C. N. Xu, and Y. Ren, *Phys. Rev. B* **71**, 052409 (2005).

[4] X. G. Zheng, H. Kubozono, K. Nishiyama, W. Higemoto, T. Kawae, A. Koda, and C. N. Xu, *Phys. Rev. Lett.* **95**, 057201 (2005).

[5] S.-H. Lee, H. Kikuchi, Y. Qiu, B. Lake, Q. Huang, K. Habicht, and K. Kiefer, *Nature Mat.* **6**, 853 (2007).

[6] J.-H. Kim, S. Ji, S.-H. Lee, B. Lake, T. Yildirim, H. Nojiri, H. Kikuchi, K. Habicht, Y. Qiu, and K. Kiefer, *Phys. Rev. Lett.* **101**, 107201 (2008).

[7] A. S. Wills and J.-Y. Henry, *J. Phys.: Condens. Matter* **20**, 472206 (2008).

[8] H. Morodomi, K. Ienaga, Y. Inagaki, T. Kawae, M. Hagiwara, X. G. Zheng, *J. Phys.: Conf. Ser.* **200**, 032047 (2010).

[9] H. Morodomi, K. Ienaga, Y. Inagaki, T. Kawae, M. Hagiwara, X. G. Zheng, *J. Phys.: Conf. Ser.* **400**, 032058 (2012).

# Effects of stabilizers on the protein-like dynamical transition of PNIPAM: a neutron scattering study

B. P. Rosi<sup>1</sup>, A. D'Angelo<sup>2,3</sup>, A. Paciaroni<sup>1</sup>, M. Zanatta<sup>4</sup>, F. Natali<sup>3,5</sup>, M. Zamponi<sup>6</sup>, D. Noferini<sup>6,7</sup>, S. Corezzi<sup>1</sup>, L. Comez<sup>8</sup>, C. Petrillo<sup>1</sup>, F. Sacchetti<sup>1</sup>, A. Orecchini<sup>1,8</sup>

<sup>1</sup> Department of Physics and Geology, University of Perugia, I-06123, Italy

<sup>2</sup> Laboratoire de Physique des Solides, CNRS, Université Paris-Saclay, 91405 Orsay Cedex, France

<sup>3</sup> Institut Laue-Langevin, 71 avenue des Martyrs, CS 20156, 38042, Grenoble, Cedex 9, France

<sup>4</sup> Department of Physics, University of Trento, I-38123 Trento, Italy

<sup>5</sup> CNR-IOM, OGG, 71 avenue des Martyrs, CS 20156, 38042, Grenoble, Cedex 9, France

<sup>6</sup> Forschungszentrum Jülich GmbH, Jülich Centre for Neutron Science at Heinz Maier-Leibnitz Zentrum, Lichtenbergstraße 1, 85747 Garching, Germany

<sup>7</sup> European Spallation Source ERIC, Box 176, SE-221 00 Lund, Sweden

<sup>8</sup> CNR-IOM c/o Department of Physics and Geology, University of Perugia, I-06123, Perugia, Italy

The dynamical transition (DT) is an ubiquitous phenomenon observed in many bio-macromolecules including proteins, DNA, and tRNA, which consists in the activation at  $T_d \approx 220$  K of anharmonic fluctuations occurring on the ps to ns time scale. Such a fast dynamics is made accessible by neutron scattering techniques, including Elastic Incoherent Neutron Scattering (EINS). The activation of anharmonic motions is accompanied with an increased macromolecular flexibility, that is deemed as necessary for biological functionality. The DT is triggered by the plasticizing effect exerted by the surrounding aqueous environment. Indeed, the transition is not observed in completely dry proteins, and hydration water itself undergoes a DT. The fundamental role of the solvent in the transition has been further explored by substituting water with stabilizing compounds. Stabilizers such as sugars and polyols are usually employed for storage of proteins, in order to preserve them against unfolding and degradation. Several studies have shown that stabilizers stiffen fast protein motions, and shift  $T_d$  toward higher values. Interestingly, a connection between the preservative action on macroscopic scales and the inhibition of the DT has been suggested, however, the details of such a microscopic interaction are still not entirely clear. Quite surprisingly, a DT in the presence of water has also been recently observed in a poly(Nisopropylamide) or PNIPAM. The latter is a simple, synthetic polymer, that is known for its ability of undergoing a reversible transition from a coil to a globule state in response to temperature variations, reminiscent of the unfolded-folded transition of proteins in aqueous solutions. The “protein-like” character of PNIPAM makes it an excellent model system for investigating the connection between solvent characteristics, macromolecular flexibility and activation of the DT. By means of EINS techniques, we studied the impact of different water/stabilizer mixtures (glycerol, glucose) on the fast dynamics of PNIPAM, over different time and length scales. Our analysis reveals a tight coupling between the dynamics of PNIPAM and that of the solvent, together with strong analogies with the protein behaviour.

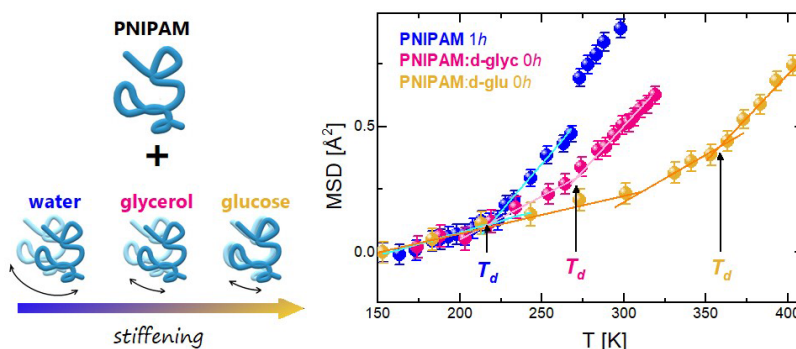


**Figure 1. Mean square displacements (MSD) on a time scale of  $\tau_R=150$  ps of PNIPAM in pure water (PNIPAM 1h), pure glycerol (PNIPAM:d-glyc 0h) and pure glucose (PNIPAM:d-glu 0h)**

[1] L. Tavagnacco et al., Phys. Rev. Res., 3 (2021) 013191.

[2] L. Tavagnacco et al., J. Phys. Chem. Lett., 10 (2019) 870-876.

[3] M. Zanatta et al., Sci. Adv., 4 (2018) eaat5895 .

# Structural and magnetic disorder in defect spin ice $\text{Ho}_2\text{Ti}_{1.5}\text{Sc}_{0.5}\text{O}_{6.75}$

***T.S. Northam***<sup>1,2</sup>, L. Mangin-Thro<sup>2</sup> and J.P. Goff<sup>1</sup>

<sup>1</sup> *Department of Physics, Royal Holloway, University of London, Egham, TW20 0EX, UK.*

<sup>2</sup> *Institut Laue-Langevin, CS 20156, 38042 Grenoble Cedex 9, France.*

Geometrically frustrated systems have been a topic of discussion for a number of years with particular interest in quantum spin liquids, states of quantum magnets in which electronic spins reside in macroscopic superpositions of infinitely many microstates, and classical spin liquids, or spin-ice, with an important example being the pyrochlore  $\text{Ho}_2\text{Ti}_2\text{O}_7$  [1]. The Ho ions of this sample are arranged in corner-sharing tetrahedra with an O ion in the centre of the tetrahedra. The ground state configuration of this material is two spins in (towards the O) and two out (away from the O). This two-in-two-out configuration is obeyed over a very long range at low temperatures, resulting in the appearance of bow tie like structures in reciprocal space called pinch points. As the temperature is increased, these pinch points broaden due to the emergence of magnetic monopoles [2], tetrahedra violating the two-in-two-out rule. Recently it has been predicted that for spin-ice materials with non-Kramers ions, such as  $\text{Ho}_2\text{Ti}_2\text{O}_7$ , it is possible to tune between classical and quantum spin liquid behaviour with long-range entanglement via the controlled introduction of structural disorder [3].

Measurements on highly defective single-crystal  $\text{Ho}_2\text{Ti}_{1.5}\text{Sc}_{0.5}\text{O}_{6.75}$  at a temperature of 50 mK were performed using the diffractometer D7 at the Institut Laue-Langevin. The capability of this instrument to use polarized neutrons was used to properly separate the magnetic and nuclear contributions. Density functional theory calculations were performed and compared with the nuclear diffuse scattering data. We find that the oxygen vacancies are on the sites at the centre of the rare-earth tetrahedra. Crystal electric field calculations using a point charge model show that for this structural defect the four neighbouring Ho ions have non-magnetic singlet ground states [4]. The magnetic diffuse scattering data showed well defined pinch points in agreement with Monte Carlo modelling and as predicted for the removal of spins from spin ice [5].

[1] T Fennell *et al.*, *Science* 326 (2009) 415-17.

[2] C Castelnovo *et al.*, *Nature* 451 (2008) 42–45.

[3] L. Savary *et al.*, *Phys. Rev. Lett.* 118 (2017).

[4] G. Sala *et al.* *Nat. Mater* 13 (2014) 488–493.

[5] A Sen *et al.*, *Phys. Rev. Lett.* 114 (2015).

# Diffusive dynamics in crowded solutions containing two types of proteins.

L. Colin<sup>1,2</sup>, C. Beck<sup>2,1</sup>, T. Seydel<sup>1</sup>, O. Matsarskaia<sup>1</sup>, F. Schreiber<sup>2</sup>

<sup>1</sup> Institut Laue – Langevin – 71 avenue des Martyrs, CS 20156, 38042 Grenoble Cedex 9, France

<sup>2</sup> Institut für Angewandte Physik, Universität Tübingen, Auf der Morgenstelle 10, 72076 Tübingen, Germany

The interior of living cells is occupied by macromolecules such as proteins, which occur at a high total volume fraction  $\phi$  on the order of 30% in the aqueous solution of the intracellular fluid. The issue of macromolecular crowding is therefore of primordial importance for the function of living cells [1]. In particular diffusion processes, which constitute a principal biological transport mechanism, are affected by crowding. In vitro, the simplest approximation to model the situation of crowding is achieved by self-crowding. In this case, the same macromolecule is used both as tracer particle and as a crowding agent in aqueous solution. Previously, we have studied self-crowding using the model proteins bovine serum albumin (BSA) [2], representing a nearly spherical shape, and bovine gamma-globulin (or: immunoglobulin) (Ig) [3], representing a strongly branched shape, in aqueous (D<sub>2</sub>O) solutions. The apparent diffusion coefficient of BSA and Ig, respectively, can each be described quantitatively with predictions from colloid theory for hard spheres [2-4,5]. In addition, we investigated the internal dynamics [6,7] of pure solutions of both proteins.

Recently, we have investigated protein mixtures containing bovine polyclonal Ig and BSA in D<sub>2</sub>O with the new optional BATS mode of IN16B (ILL). The high energy resolution and high energy transfers in combination with the known sample composition allowed us to separate both apparent global diffusion coefficients of Ig and BSA as well as the internal dynamics of the proteins. The high energy transfers, accessible with the BATS option, allow to separate in addition also the dynamics of the backbone and the side chains [8] (see Figure 1).

Significant deviations of the apparent global diffusion coefficients from the single pure protein solution are observed in the protein mixtures. The bigger protein Ig is slowed down due to the presence of BSA, while the latter one is accelerated compared to the situation of monodisperse crowding. A monotonous trend of the deviation of the diffusion coefficient from the one in pure solution at same total volume fraction as a function of the protein percentage of the total volume fraction can be observed. This deviation vanishes in the limit where the second protein concentration goes to zero. These results are in agreement with Stokesian simulations performed in the context of NBS studies investigating the diffusion of proteins in a cell-like environment [9]. They predict an acceleration or a slowing-down of proteins being smaller or bigger, respectively, than the averaged particle size in solution compared to the monodisperse case at the same total volume fraction.

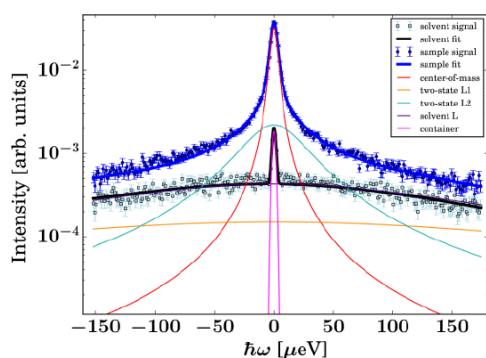


**Figure 1.** Example spectrum recorded on BATS,  $q=1.2 \text{ \AA}^{-1}$  on a solution of pure Ig in D<sub>2</sub>O (upper dark symbols) and pure D<sub>2</sub>O signal (lower light symbols, container contribution not subtracted). The red line represents the center-of-mass diffusion in the fit. The orange and cyan lines denote the two internal diffusion components arising from protein backbone and side chain motions, respectively [5,8].

- [1] R.J. Ellis; Curr. Opin. Struct. Biol. 2001, 11, 114–119.
- [2] F. Roosen-Runge, et al; PNAS 2011, 108, 11815.
- [3] M. Grimaldo, et al J.Phys.Chem.B 2014, 118, 7203.
- [4] A.J. Banchio, et al J. Chem. Phys. 2008, 128, 104903.
- [5] M. Grimaldo, et al Quart. Rev. Biophys. 52 (2019) e7, 1
- [6] M. Grimaldo, et al Phys.Chem.Chem.Phys. 2015, 17, 4645.
- [7] M. Grimaldo, et al J. Phys. Chem. Lett. 2019, 10, 1709.
- [8] F. Roosen-Runge et al, J.Chem.Phys. 2016, 144, 204109
- [9] C. Beck, et al J.Phys.Chem.B 2018, 122, 8343.

# Neutron Diffraction Study of NaMgD<sub>3</sub> at High Pressure

*Julius Andrew Nunez*, Céline Goujon, Salvatore Miraglia, Claire Colin, and Laetitia Laversenne  
*Université Grenoble Alpes, CNRS, Institut Néel, 38000 Grenoble France*

Sodium magnesium hydride, NaMgH<sub>3</sub>, was found to have 6.0% by mass of hydrogen released at 673 K within 8 minutes[1]. This sparked future investigations on the material for hydrogen storage applications. Due to problems concerning thermodynamics and kinetics, this material's hydrogen sorption property is expected to be improved by modifying the material through cation substitution or by high-pressure processing. The aim is to investigate the behavior of NaMgH<sub>3</sub> at high pressure.

The sample was synthesized using the CONAC Press at 4 GPa, 650°C for 2 h. Deuteration of the sample to produce NaMgD<sub>3</sub> was performed in an autoclave under 40 bars hydrogen at 325°C for 8 days. Neutron diffraction was performed at the D1B beamline of the Institut Laue-Langevin, Grenoble, France using a Paris-Edinburgh Press set-up with NaCl as the pressure calibrant. Patterns were collected at 300 K with a wavelength of 2.52 Å at different pressures up to 10.7 GPa.

Diffraction patterns showed lattice compression and no phase transition at room temperature for the pressure range investigated. Using pressure values from NaCl calibration and the obtained lattice parameters for NaMgD<sub>3</sub>, a fit using the third order Birch-Murnaghan Equation of State was performed and gave  $B_0 = 45.2$  GPa and  $B_0' = 2.9$ . Results are to be compared with Li-substituted NaMgD<sub>3</sub> samples in future beamtimes.

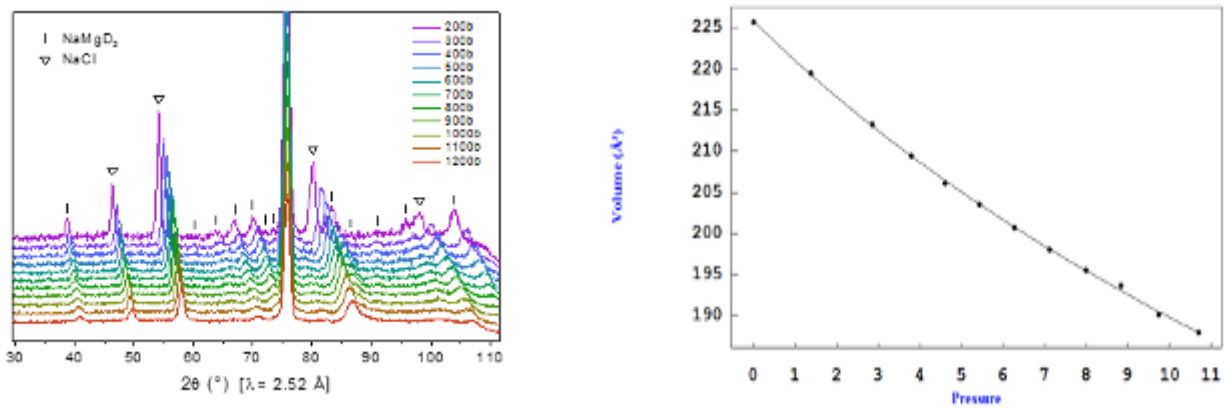


**Figure 1. Neutron diffraction patterns (top) of NaMgD<sub>3</sub> up to ~10.7 GPa and the corresponding change in unit cell volume (bottom).**

[1] Ikeda K, Kogure Y, Nakamori Y and Orimo S 2005 Reversible hydriding and dehydriding reactions of perovskite-type hydride NaMgH<sub>3</sub> *Scr. Mater.* **53** 319–22

# Picosecond dynamics of polymorphs of lysozyme aggregates with different levels of cytotoxicity

T. Matsuo<sup>1,2,3</sup> and J. Peters<sup>1,2</sup>

<sup>1</sup> Univ. Grenoble Alpes, CNRS, Laboratoire Interdisciplinaire de Physique (LiPhy), 140 rue de la physique, 38402 Saint Martin d'Hères, France

<sup>2</sup> Institut Laue-Langevin, 71 avenue des Martyrs, CS 20156, 38042 Grenoble Cedex 9, France

<sup>3</sup> Institute for Quantum Life Science, National Institutes for Quantum and Radiological Science and Technology (QST), 2-4 Shirakata, Tokai, Ibaraki, 319-1106, Japan

Lysozyme amyloidosis is a hereditary severe disease, where lysozyme amyloid deposits in liver and kidney cause massive hemorrhage, resulting in the death of a patient. Amyloid fibrils are self-assembled protein filaments with core regions rich in  $\beta$ -sheet. It has been shown that lysozyme fibrils show structural polymorphism depending on fibrillation conditions and each polymorph shows different levels of cytotoxicity: fibrils formed at neutral pH are more cytotoxic than those formed at acidic pH [1–3]. Cytotoxicity originates from interactions between fibrils and cell membranes. In particular, it is the amino acid side-chains of the fibrils that directly interact with the components of the membranes. It is thus important to characterize the mobility of side-chains of lysozyme polymorphs to gain insights into the molecular mechanism of cytotoxicity.

In this study, we focused on the polymorphism of hen egg white lysozyme (HEWL), a model for studying lysozyme amyloidosis in humans and prepared D<sub>2</sub>O hydrated powder samples of two HEWL amyloid polymorphs formed at pH 6.0 (hereafter called Fib6) or 2.7 (Fib2), which are known to show higher and lower levels of cytotoxicity, respectively. We carried out elastic incoherent neutron scattering (EINS) measurements on these samples using the IN13 spectrometer at Institut Laue-Langevin in France in the temperature range from 20 K to 310 K. In the first analysis, temperature dependences of the mean square displacements (MSDs) of atomic motions in the proteins were evaluated from the EINS spectra. There were, however, no significant differences in the extracted MSD values between the two samples in the temperature range studied albeit the difference in the shape of the EINS curves. Next, analysis based on the mean square positional fluctuations (MSPFs) [4] was conducted, which uses all the data points in the EINS curves and thus provides more detailed dynamical information than the MSD analysis. It was found that whereas the MSPF values of atomic motions are similar between the two samples, each polymorph shows a different degree of motional heterogeneity: Fib6 showed a larger fraction of atoms undergoing motions with larger amplitudes than Fib2. Furthermore, application of the Bicout-Zaccai model [5] showed that  $\Delta G$  of atomic motions tends to be lower for Fib6, suggesting that the energy barrier of atomic motions is lower for Fib6. These results suggest that the differences in molecular dynamics between lysozyme polymorphs lie in the distribution of local atomic motions and these dynamical differences would modulate the way by which the polymorphs interact with cell membranes, contributing to the differences in the level of cytotoxicity.

[1] Mossuto et al., J. Mol. Biol. 402 (2010) 783–796.

[2] Mocanu et al., Int. J. Biol. Macromol. 65 (2014) 176–187.

[3] Sulatskaya et al., J. Mol. Struct. 1140 (2017) 52–58.

[4] J. Peters and G. Kneller, J. Chem. Phys. 139 (2013) 165102.

[5] D. Bicout and G. Zaccai, Biophys. J. 80 (2001) 1115–1123.

# Implementation of in-situ neutron characterization techniques for the characterization of metal additive manufacturing

**B. Ozcan**<sup>1</sup>, S. Cabeza<sup>1</sup>, T. Pirling<sup>1</sup>, T. C. Hansen<sup>1</sup>, J. Cormier<sup>2</sup>, S. Polenz<sup>3</sup>, E. López<sup>3</sup>, C. Leyens<sup>3,4</sup>

<sup>1</sup> Diffraction Unit, Institute Laue Langevin, ILL, 71 Avenue des Martyrs, 38042 Grenoble, France.

<sup>2</sup> Institut Pprime, UPR CNRS 3346, ISAE-ENSMA, 1 avenue Clément Ader, BP 40109, 86961 Futuroscope-Chasseneuil, Poitiers, France.

<sup>3</sup> Additive Manufacturing Division, Fraunhofer IWS, Winterbergstraße 28, 01277 Dresden, Germany.

<sup>4</sup> TU Dresden, Institute of Materials Science (IfWW), D-01062, Dresden, Germany.

The fundamental relationship between strain formation and process parameters during additive manufacturing (AM) is a key point for the controlling of mechanical properties in AM engineering parts and their applications. Throughout the AM process, complex thermal gradients, microstructure, and residual stress gradients within the bulk play a critical role in the later mechanical response of the component<sup>1</sup>. Furthermore, these properties evolve as a function of time, temperature, build height, and processing parameters. An assessment can be performed to investigate the final condition of the engineering part with ex-situ strain studies including lab-scale characterization and numerical modeling techniques, however, strain evolution during AM cannot be yet accurately estimated contrary to conventional manufacturing techniques such as casting, forging, and welding. Additionally, some aspects of ex-situ studies may remain unanswered due to the lack of information on AM strain mechanisms. Therefore, in-situ studies are highly attractive for providing a better understanding of dynamic evolution of strain mechanisms. In this context, an in-situ neutron strain monitoring during direct energy deposition (DED) of Inconel 718 (IN718) was carried out at SALSA beamline at Institut Laue Langevin (ILL), France<sup>2,3</sup>. During this study, the shift in Bragg angle ( $2\theta^\circ$ ) of Ni(311) peak was continuously monitored during printing and cooling periods. The results were rationalized in 3 categories (thermal, microstructural, and residual stress-based contribution) depending on (i) measurement locations in horizontal direction regarding melt pool: *Melt pool center*, *10 and 30 mm on the back of the melt pool track*, (ii) region of interest in vertical direction regarding melt pool: *Melt pool area* (0 – 2 mm), *Near-melt pool area* (2 – 4 mm), and *Far-field area* (4 – 8 mm), and finally, (iii) time to print a layer vs peak fitting quality. As expected, the material showed a time, build height, and most remarkably processing region dependency throughout the printing. As a complementary study to understand the precipitation & dissolution kinetics of the IN718 AM alloy, a continuous observation on phase evolution during heat treatments was performed at the D20 beamline at ILL. The early results show the evolution of Ni- $\gamma$  matrix peaks in time and temperature with incipient precipitation of secondary phases such as hexagonal Laves –  $(\text{Ni,Cr,Fe})_2(\text{Nb,Mo,Ti})$  and strengthening phases fcc  $\gamma'$ -Ni<sub>3</sub>(Al,Ti) and bct  $\gamma''$ -Ni<sub>3</sub>Nb<sup>4</sup>. These results can be implemented in the previous in-situ study for developing a better approach to microstructural contribution to total strain.

Overall, these neutron research approaches enhance the optimization of residual stress and secondary phase precipitations of IN718 and serve as complementary studies to lab-scale mechanical and microstructural characterization techniques.

[1] Popovich, V. A. et al. Mater. Des. 114, (2017), 441–449

[2] Lopez, E. et al. (2018)

[3] Cabeza, S. et al. Superalloys 2020, (2020), 1033–1045

[4] Zhang, D. et al. Mater. Sci. Eng. A 644, (2015), 32–40

# Monitoring food structure in plant protein gels during digestion: from rheometry to Small Angle Neutron Scattering

*M. Napieraj*<sup>1</sup>, F. Boué<sup>1</sup>, E. Lutton<sup>2</sup>, and A. Brûlet<sup>1</sup>

<sup>1</sup> LLB, CEA Saclay

<sup>2</sup> INRAE-MIA Paris

Proteins are essential macronutrients in the human diet, being fundamental in body structure and functions. The protein digestibility depends not only on their composition but also on food structure, which in turn can be influenced by different types of processing. We monitored degradation kinetics of the structure during simulated gastric and intestinal digestion. As a model solid-like food (the form in which most proteins are ingested) we used plant protein gels - from rapeseed (napin and cruciferin). The gels were synthesized by heat-treatment of solutions at various concentrations and pHs. Different techniques were used. We will focus here on SANS, on 1cm size samples as in real digestion bolus, but which need to be homogeneous. SAXS (LLB and SWING-SOLEIL synchrotron) gives additional information at the same  $q$  values but not the same size of samples, enabling infra-millimetric access to the spatial gradient. We also used UV fluorescence imaging (DISCO) at intermediate gel size (20-200 microns). We make a link with rheological measurements. The SANS can be separated in two regimes of  $q$  (Figure 1): a low  $q$  one corresponding to the signal of aggregated proteins, a high  $q$  one corresponding to the scale of the individual proteins: disappearance, unfolding-refolding. The corresponding protein conformation is better seen using the Kratky representation (Insert), in particular the existence of a maximum typical of a compact object, together with a slope around 2 (meaning initially  $I(q) \sim q^{-2}$ ). The state of gelled proteins defines both (i) their intrinsic digestibility and (ii) the gel structure. As a concrete example, unfolding can make digestion easier and the proteins more entangled, possibly leading to a higher modulus. As digestion proceeds, we observe complex combinations, like unfolding-refolding-unfolding. This is illustrated in the exponent vs correlation length diagram (Figure 2), where one gastric digestion corresponds to a kind of loop (red curve), while intestinal digestion following about 30 min of gastric digestion leads to compact and small aggregates.

A new step currently developed is to separate the influence of digestion on the state of the proteins in the network strands (e. g. due to unfolding) from the modification of the gel structure. We will introduce the protein inside a gel of polygalacturonane (PGA from pectin), not digestible by human enzymes, and match the scattering length of PGA or the protein.

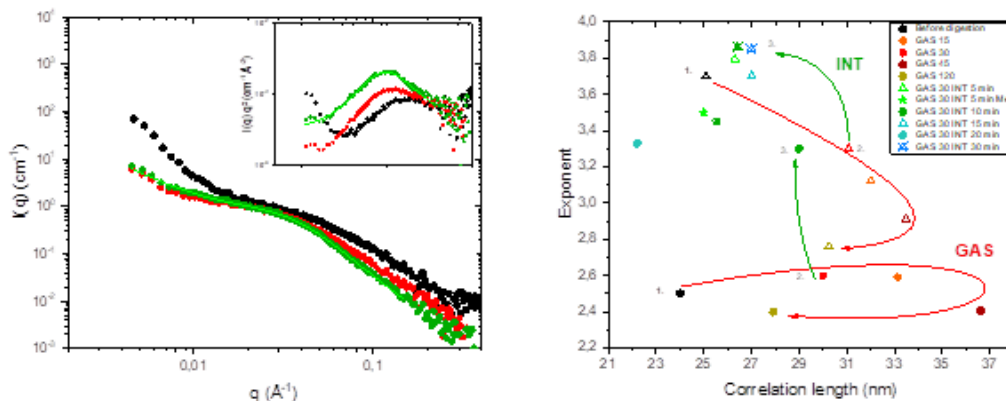


**Figure 1. (left) Scattered intensity versus  $q$  for three conditions: non digested, 30 min gastric + ... min intestinal, 30 min gastric + ... min intestinal. (right) Diagram for the high  $q$  behaviour: high  $q$  exponent versus high  $q$  correlation length. The arrows link all samples with the first initial gel preparation.**

[1] Pasquier, J. et al., Colloids and Surfaces A 570 (2019) 96–106.

[2] Napieraj, M. et al., to be submitted.

# Exploring the D–Hf phase diagram using in-situ neutron diffraction

*M. Dottor*<sup>1</sup> and J.-M. Joubert<sup>1</sup>

<sup>1</sup> *Univ Paris Est Créteil, CNRS, ICMPE, UMR 7182, 2 rue Henri Dunant, 94320 Thiais, France*

H-Hf phase diagram knowledge is a key to understand and solve technical issues. In the next fast reactors, hafnium hydride can be used as control rods [1] and very recently, the use of hafnium with palladium has shown its usefulness for optical hydrogen sensors [2].

This phase diagram contains four different phases: the hexagonal phase  $\alpha$ -Hf, the distorted cubic phase  $\delta'$ -HfD<sub>2-x</sub>, the cubic phase  $\delta$ -HfD<sub>2-x</sub> and the tetragonal phase  $\epsilon$ -HfD<sub>2</sub> which are shown in Figure 1. However, the phase diagram is only partially known, assumptions have been made to draw this diagram and thus, the phase transitions are still not well established. Additionally, the existence of the tetragonal phase  $\gamma$ -HfD (*P4<sub>2</sub>/mmc*) was recently predicted by ab-initio calculations [2].

We will present our results obtained on the deuteration of hafnium during one experiment conducted at ILL on D1B [3]. Firstly, our experiment clarified the existence or not of the  $\gamma$ -HfD phase. Therefore, we have established the stability, the structure and the site occupancies of D and Hf of this phase. Moreover, we also investigated the range of existence of all the phases of this phase diagram; either during increasing and decreasing the temperature at known composition or during the isothermal study by varying the composition in deuterium. Thus, the particularity and originality of this work lies in the in-situ study of both composition and temperature of this phase diagram.

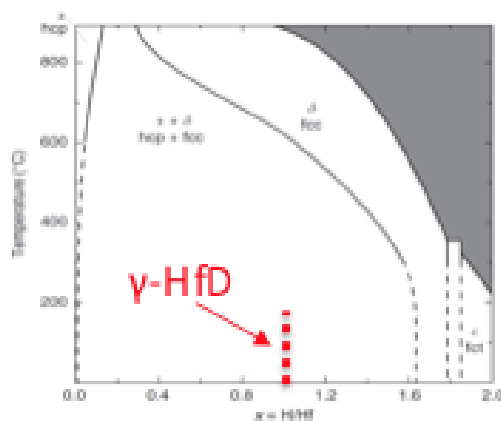


Figure 1. Phase diagram of H-Hf system taken from Boelsma et al. [2].

[1] Boelsma, C.; Bannenberg, L. J.; van Setten, M. J.; Steinke, N.-J.; van Well, A. A.; Dam, B. *Nat. Commun.* 8 (2017) 15718. <https://doi.org/10.1038/ncomms15718>.

[2] Bourgeois, N.; Crivello, J.-C.; Cenedese, P.; Joubert, J.-M. *ACS Comb. Sci.* 19, 8 (2017) 513–523. <https://doi.org/10.1021/acscombsci.7b00050>.

[3] Dottor, M.; Couturas, F.; Crivello, J.-C.; Joubert, J.-M.; Laversenne, L.; Nassif, V.; Puente Orench, I. Study of the D-Hf Phase Diagram Using in-Situ Neutron Diffraction (2021). <https://doi.org/10.5291/ILL-DATA.CRG-2812>.

# Insertion and activation of functional bacteriorhodopsin in a floating bilayer

*Tetiana Mukhina*<sup>1,2,3</sup>, Yuri Gerelli<sup>1,4</sup>, Arnaud Hemmerle<sup>5</sup>, Jean Daillant<sup>5</sup>, Thierry Charitat<sup>2</sup>, *Giovanna Fragneto*<sup>1</sup>

<sup>1</sup> Institut Laue-Langevin, 71 av. des Martyrs, BP 156, 38042 Grenoble Cedex, France

<sup>2</sup> Institut Charles Sadron, Université de Strasbourg, CNRS, UPR 22, 67034 Strasbourg, France

<sup>3</sup> Institute for Condensed Matter Physics, TU Darmstadt, Hochschulstrasse 8, 64289 Darmstadt, Germany

<sup>4</sup> Marche Polytechnic University, Department of Life and Environmental Sciences, Via Breccia Bianche, 60131 Ancona, Italy

<sup>5</sup> Synchrotron SOLEIL, L'Orme des Merisiers, Saint-Aubin, BP 48, F-91192 Gif-sur-Yvette Cedex, France

Lipid bilayer serves as an excellent platform for biological and physical studies and comprise a suitable model system to probe protein-membrane and membrane-membrane interactions. By itself cell membrane exhibits thermal fluctuations that can be enhanced by transmembrane protein activity leading to out-of-equilibrium fluctuations. Active fluctuations have been widely described theoretically [1], but to a lesser extent experimentally.

We will present our recent results on the development of a robust and reproducible protocol for transmembrane protein reconstitution into planar solid-supported single and floating phospholipid bilayers in gel and fluid phases by applying a detergent-mediated incorporation method [2]. In this context, bacteriorhodopsin was used as a light-driven proton pump, whose activity can be triggered by visible light.

A wide range of surface-sensitive techniques such as QCM-D, AFM, fluorescence microscopy, neutron and X-ray reflectometry was used in order to confirm and optimize protein incorporation. Incubation time, protein and detergent concentration as well as lipid composition were optimized in order to preserve membrane structural integrity and protein activity. By means of scattering techniques, the structure and composition of this membrane-protein system before and after protein reconstitution at sub-nanometer resolution were resolved. It was shown that lipid bilayer integrity and protein activity were preserved upon the insertion process. Reversible structural modifications of the membrane, induced by the bacteriorhodopsin functional activity triggered by visible light, were observed and characterized at the nanoscale. In particular, changes in structure and composition of the floating bilayer upon sample illumination were consistent with an enhancement of out-of-equilibrium membrane fluctuations induced by the light-activated protein pumping activity [3].

This result opens new outstanding perspectives as the investigation of the active fluctuation spectrum of floating bilayer systems with embedded bacteriorhodopsin and opens access to physical properties of the system such as bending modulus, surface tension and interaction potential between adjacent membranes.

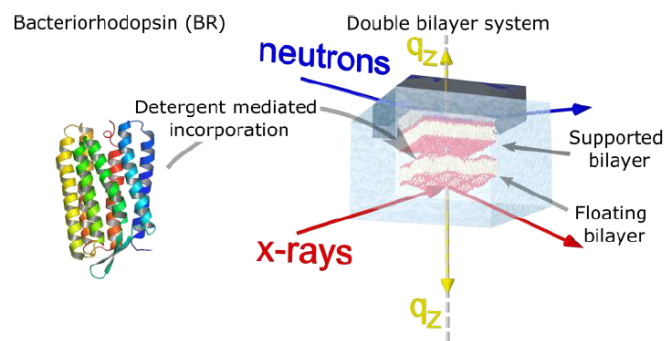


**Figure 1. Ternary structure of BR and schematic illustration of a double lipid bilayer system alongside a representation of the scattering geometry for reflectometry experiments.**

[1] Prost J., Manneville J.-B., and Bruinsma R., EPJ B (1998) 1:465–480

[2] Dezi M., Di Cicco A., Bassereau P. and Lévy D., PNAS (2013) 110 (18) 7276-7281

[3] Mukhina T. et al., J. Colloid Interface Sci. 597 (2021) 370–382

Abstracts for  
Wednesday 22th of september

# Loop currents in quantum matter

*P. Bourges*<sup>1</sup>

<sup>1</sup> *Laboratoire Léon Brillouin, CEA-CNRS UMR12 91191 Gif-sur-Yvette Cedex, France*

In many quantum materials, strong electron correlations lead to the emergence of new states of matter. In particular, the study in the last decades of the complex phase diagram of high temperature superconducting cuprates highlighted intra-unit-cell electronic instabilities breaking discrete Ising-like symmetries, while preserving the lattice translation invariance [1]. Polarized neutron diffraction experiments have provided compelling evidences supporting a new form of intra-unit-cell magnetism, emerging concomitantly with the so-called pseudogap state of these materials. This observation is currently interpreted as the magnetic hallmark of an intra-unit-cell loop current order, breaking both parity and time-reversal symmetries. In this talk, I will review this magneto-electric state, likely to exist in a wider class of quantum materials beyond superconducting cuprates. For instance, it has been already observed in hole-doped Mott insulating iridates or in the spin liquid state of hole-doped 2-leg ladder cuprates [2].

[1] P. Bourges, D. Bounoua, and Y. Sidis, <https://arxiv.org/abs/2103.13295> to appear in C.R. Physique (2021).

[2] D. Bounoua et al, Comm. Phys, 2, 123 (2020).

# In situ study of energy materials by neutron diffraction

L. Laversenne <sup>1</sup>

<sup>1</sup> Univ. Grenoble Alpes, CNRS, Grenoble INP, Institut Néel, 38000 Grenoble, France

One of the advantages of neutrons is their high penetration depth which allows the use of complicated sample environments hence enabling to characterize materials under very diverse experimental conditions. Such experiments are conducted on the rather old but still robust and reliable CRG-D1b diffractometer at ILL where temperature-, pressure-, or magnetic field-dependent phase transitions are frequently investigated. In this contribution, will be presented two examples of *in situ* studies in which thermodiffractometry is combined with an ancillary equipment to unveil transformation pathways in energy materials.

The first study concerns the investigation of hydrogen sorption properties in magnesium based composite materials. These Mg-Mg<sub>2</sub>Ni composites have been processed by forging and exhibit remarkable sorption kinetics. Neutron powder diffraction was performed in the course of successive absorptions and desorptions while monitoring the deuterium pressure in the sample holder. The combined measurements allowed to identify the sequence of phases that formed and to determine the mechanism of transformations from the metal state to the hydride and vice versa.

The second investigation is about magnesium sulfate heptahydrate (aka epsomite) considered as a candidate for seasonal energy storage systems. In particular, we will describe the multiple steps of the dehydration of the deuterated salt MgSO<sub>4</sub>.7D<sub>2</sub>O. For this purpose, simultaneous structural analysis and gravimetric measurements were carried out with the thermobalance developed by the CRG- D1b team. The mass losses recorded during the heating of the compound were correlated to the structural transitions (cf. figure 1) and confronted with the available literature data for the MgSO<sub>4</sub>- H<sub>2</sub>O system. One remarkable input is the highlighting of several non-stoichiometric hydrates formed in the course of dehydration.

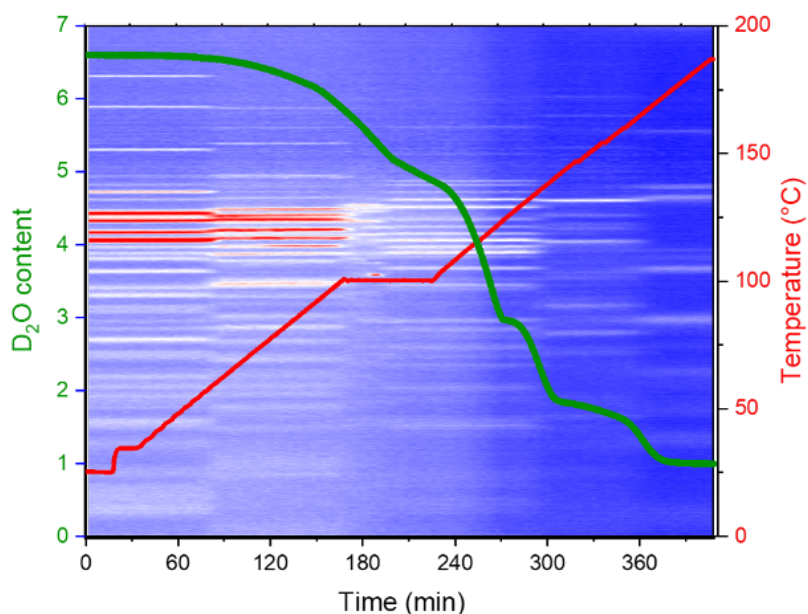


Figure 1: Combined NPD and gravimetric measurements collected in the course of dehydration of epsomite.

# Following surfactant assemblies in foams

A. Salonen<sup>1</sup>

<sup>1</sup> *Laboratoire de Physique des Solides, CNRS, Univ. Paris-Sud, Université Paris-Saclay 91405 Orsay cedex, France*

Dispersing gas in a liquid makes foam. Foams are present in an enormous range of products largely because of their interesting mechanical and conductive properties. These properties arise because of the structure of foams, which are made of interconnected liquid channels bounded by gas/water interfaces. The stability and properties of the foams are intricately controlled by the properties of, both the interfaces and the liquid channels. Therefore, it is important to understand the organisation of both. Small angle neutron scattering is an excellent tool to probe the local structure of the stabilising molecules at the interfaces and in the surrounding solution [1].

We have studied the stability of foams made with surfactant assemblies, with a particular emphasis in following the assembly structures inside the foams using small angle neutron scattering. Mixtures of cationic and anionic surfactants have rich phase behaviour. We have used a mismatch in hydrocarbon chain lengths to study the role of self-assembly structure on the stability of foams [2]. Alternatively, we can create ultrastable foams, when the surfactant is crystallised into particles, which block ageing at the bubble surfaces and the water channels, as seen in Figure 1 [3].

We want to create foams with perfectly controlled properties, to do this we must understand the link between molecular organisation and foam stability, which can be best probed using neutrons.

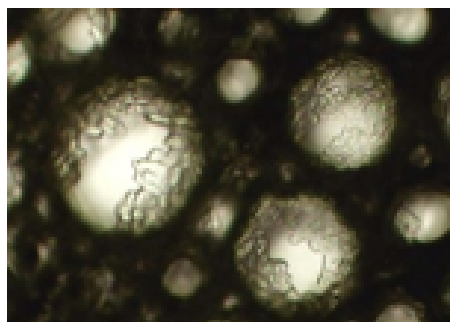


Figure 1: Crystallised surfactant particles on bubble surfaces.

[1] A. Mikhailovskaya; L. Zhang; F. Cousin; F. Boué; P. Yazhgur; F. Muller; C. Gay; A. Salonen *Adv. Colloid Interface Sci.* 2017, 247.

[2] J. Ferreira; A. Mikhailovskaya; A. Chenneviere; F. Restagno; F. Cousin; F. Muller; J. Degrouard; A. Salonen; F. E. Marques *Soft Matter* 2017, 13.

[3] L. Zhang; A. Mikhailovskaya; P. Yazhgur; F. Muller; F. Cousin; D. Langevin; N. Wang; A. Salonen *Angew. Chemie - Int. Ed.* 2015, 54.

# Unforeseen combination of magnetism and superconductivity in the pressurized $\text{BaFe}_2\text{Se}_3$ spin ladder

W.G. Zheng<sup>1</sup>, V. Balédent<sup>1</sup>, C. Colin<sup>2</sup>, F. Damay<sup>3</sup>, J.-P. Rueff<sup>4</sup>, A. Forget<sup>5</sup>, D. Colson<sup>5</sup>, and P. Foury- Leyeikian<sup>1</sup>

<sup>1</sup> Laboratoire de Physique des Solides, CNRS, Univ. Paris-Sud, Université Paris-Saclay 91405 Orsay cedex, France

<sup>2</sup> Institut Néel, CNRS UPR~2940, 25 av. des Martyrs, 38042 Grenoble, France

<sup>3</sup> Laboratoire Léon Brillouin, CEA-CNRS UMR12 91191 Gif-sur-Yvette Cedex, France

<sup>4</sup> Synchrotron SOLEIL, L'Orme des Merisiers, BP 48 St Aubin, 91192 Gif-sur-Yvette, France

<sup>5</sup> SPEC, CEA, CNRS-UMR3680, Université Paris-Saclay, Gif-sur-Yvette Cedex 91191, France

It has been recently observed that a superconducting phase emerges under pressure in the Fe-based spin-ladders  $\text{BaFe}_2\text{X}_3$  ( $\text{X}=\text{Se},\text{S}$ ) [1-3]. The low dimensionality of their lattice promises the simplification of theoretical models and a better understanding of the mechanism of superconductivity. We investigate here the frontier between magnetic and SC phases in  $\text{BaFe}_2\text{Se}_3$  by performing challenging powder neutron diffraction and Fe  $\text{K}\beta$  x-ray emission spectroscopy under high pressure. We show that the ambient pressure ground state with a unique block-like magnetic order [fig. 1(c)] is destabilized under pressure. We evidence a new pressure induced antiferromagnetic stripe-like spin order [fig. 1(d)] above 4 GPa, similar to the magnetic order of the parent superconductor  $\text{BaFe}_2\text{S}_3$  [1]. This result makes the stripe order a prerequisite for the stabilization of superconductivity in Fe-based spin ladders. This very new archetype of superconductor can pave the way to further theoretical research efforts.

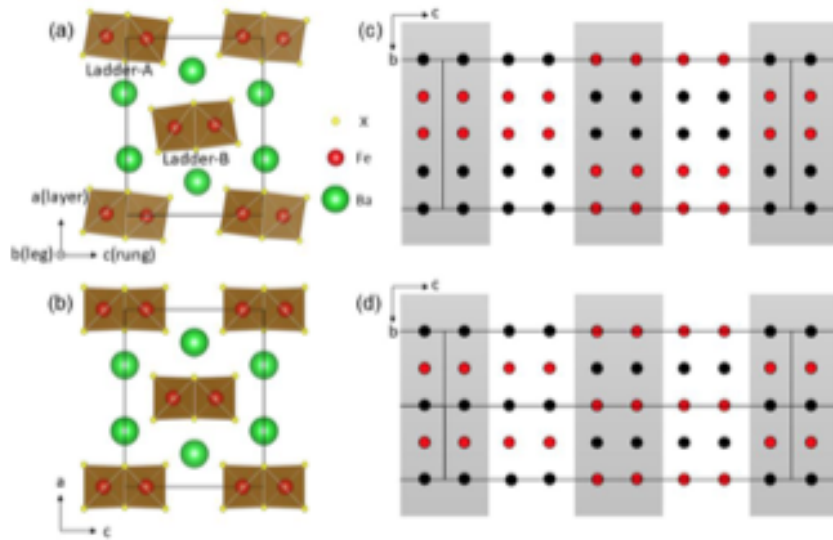


Figure 1: (a) and (b) The atomic structures of  $\text{BaFe}_2\text{X}_3$  ( $\text{X}=\text{Se},\text{S}$ ) viewed along  $b$ -axis in  $Pnma$  and  $Cmc2m$  space groups, respectively. There are two ladders (Ladder-A and Ladder-B) in each unit cell. (c) and (d) The projections of Fe spins on the  $bc$ -planes of the block-like and stripe-like magnetic orders. The moments are along the  $a$ -axis. The red and black circles correspond to the up and down spin directions of Fe, respectively. The black lines indicate the edge of the magnetic unit cell. The two different Fe ladders are separated by different background colors, White for Ladder-A and gray for Ladder-B.

[1] H. Takahashi et. al., Nature Materials, 14 (2015) 1008. [2] J. Ying et. al., Physical Review B, 24 (2017) 241109.

[2] J.M. Caron et. al., Physical Review B, 18 (2011) 180409.

# Revealing the nature of $\pi \cdots H - O$ weak interaction via neutron total scattering

C. Di Mino<sup>1</sup>, N. T. Skipper<sup>1</sup>

<sup>1</sup>Department of Physics and Astronomy, University College, Gower St, London WC1E 6BT.

The nature of alcohol-hydrocarbon interactions is of both practical and fundamental interest due to their importance in understanding biological processes (e.g., protein and DNA folding, olfactory processes etc.), supramolecular chemistry (e.g., molecular self-assembly), and gasoline purification, particularly regarding the methanol economy [1]. In addition to Van der Waals interactions, the pi systems in unsaturated hydrocarbons introduce the possibility of forming so-called 'weak' hydrogen bonds with alcohols. While weak hydrogen bonding of aromatic pi systems has been extensively studied, the even weaker interactions with alkenes make them more challenging to probe using conventional spectroscopic techniques.

Here, total neutron scattering combined with isotopic substitution has been exploited to reveal the nature of the interaction between a range of pi systems - aromatics, cyclic, and linear alkenes - and hydroxyl group in the liquid state.

By varying geometry, electron density and flexibility of the hydrocarbons, we uncover the intrinsic nature, intensity, and directionality of the interaction [2].

The systems have been modelled via EPSR simulations [3] using three different charge models, showing three different structural results. The work presented highlights the importance of the choice of seed parameters in EPSR simulations which cannot rely entirely on the refinement performed by EPSR for systems of this kind.

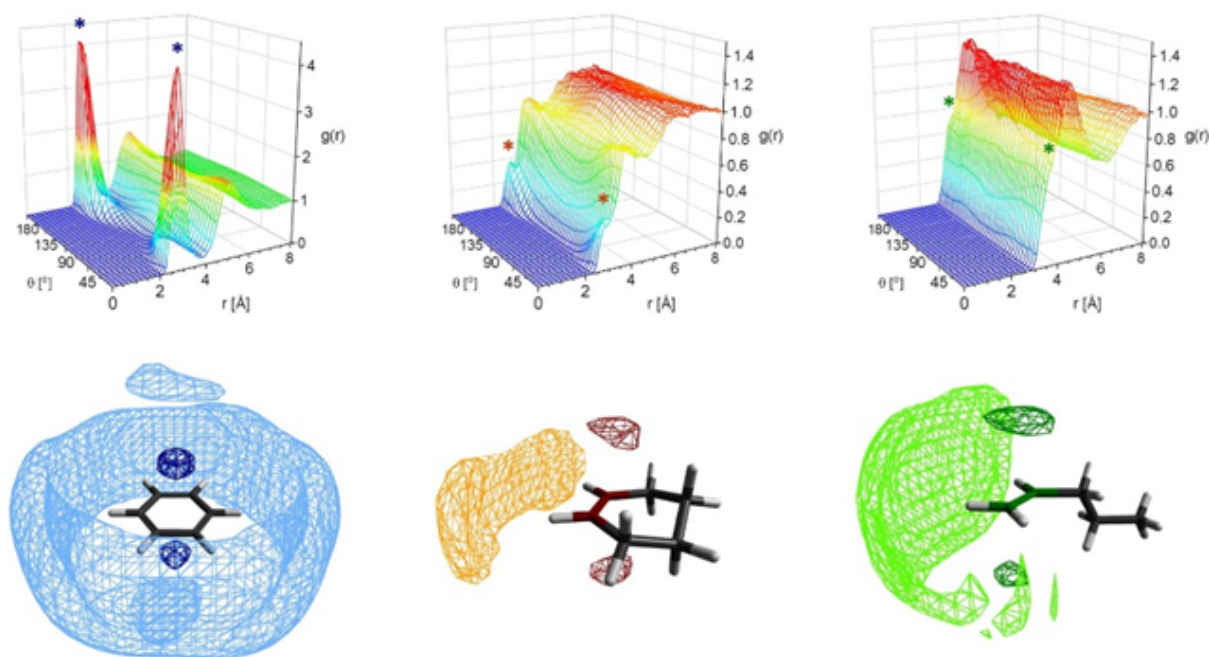


**Figure 1. Angular Radial Distribution Functions (Top) and Spatial Distribution Functions (Bottom) for the best fit model showing a weak and highly directional interaction for cyclohexene and pent-1-ene.**

[1] Olah, George A. "Beyond oil and gas: the methanol economy." *Angewandte Chemie* 44.18 (2005): 2636-2639.

[2] Heger, Matthias, Ricardo A. Mata, and Martin A. Suhm. "Soft hydrogen bonds to alkenes: the methanol-ethene prototype under experimental and theoretical scrutiny." *Chemical Science* 6.7 (2015): 3738-3745.

[3] Soper, A. K. "Empirical potential Monte Carlo simulation of fluid structure." *Chemical Physics* 202.2-3 (1996): 295-306.

# Advanced magnetocaloric materials for adiabatic demagnetization: Spin dynamics of the quantum dipolar magnet $\text{Yb}_3\text{Ga}_5\text{O}_{12}$

E. Lhotel<sup>1</sup>, E. Riordan<sup>1</sup>, L. Mangin-Thro<sup>2</sup>, E. Ressouche<sup>3</sup>, P. Steffens<sup>2</sup>, E. Bichaud<sup>4</sup>, G. Knebel<sup>4</sup>, J.-P. Brison<sup>4</sup>, C. Marin<sup>4</sup>, S. Raymond<sup>3</sup> and M. Zhitomirsky<sup>4</sup>

<sup>1</sup> *Institut Néel, CNRS et Univ. Grenoble Alpes, 38000 Grenoble, France*

<sup>2</sup> *Institut Laue Langevin, 38042 Grenoble, France*

<sup>3</sup> *Univ. Grenoble Alpes, CEA, IRIG, MEM, MDN, 38000 Grenoble, France*

<sup>4</sup> *Univ. Grenoble Alpes, Grenoble INP, CEA, IRIG, PHELIQS, 38000 Grenoble, France*

Geometrical frustration typically suppresses conventional magnetic ordering and may stabilize exotic phases with unconventional spin excitations. Apart from fundamental interest, the delayed magnetic ordering in conjunction with a large unfrozen entropy makes frustrated materials good candidates for low temperature magnetic cooling [1]. The developing space applications and increasing costs of helium motivate a continuing search for new refrigerant materials for adiabatic demagnetization refrigeration in the 0.1 - 4 K temperature range [2]. In this context, we investigate ytterbium gallium garnet,  $\text{Yb}_3\text{Ga}_5\text{O}_{12}$ . In the cubic garnet crystals, the rare earth ions form two interpenetrating lattices of cornersharing triangles often called hyperkagome lattices. An enhanced magnetocaloric effect is evidenced below 2 K in  $\text{Yb}_3\text{Ga}_5\text{O}_{12}$  [3] in the paramagnetic phase above the supposed magnetic transition at  $T_\lambda \approx 54$  mK.

Our study combines susceptibility and specific heat measurements with neutron scattering experiments and theoretical calculations [4]. Below 500 mK, the building of magnetic correlations manifests through an elastic neutron response strongly peaked in momentum space. Along with this, the inelastic spectrum develops flat excitation modes. In magnetic field, the lowest energy branch follows a Zeeman shift in accordance with the field dependent specific heat data. An intermediate state with spin canting away from the applied field direction is evidenced in small magnetic fields with a maximum effect at 0.15 T. The total magnetization almost saturates in a field of 2 T and the measured excitation spectrum is well reproduced by a spin-wave calculations taking into account solely the dipole-dipole interactions. The small positive Curie-Weiss temperature  $q_p = 97$  mK derived from the susceptibility measurements is also accounted for by the dipole spin model.

Ytterbium gallium garnet provides thus an interesting example of a quantum dipolar magnet on the hyperkagome lattice. Further experimental and theoretical investigations of the spin dynamics are necessary to elucidate the interplay between its highly symmetric frustrated geometry and the long-range dipolar interactions. In addition, the obtained results confirm that strong spin correlations in a frustrated geometry can enhance the magnetocaloric response. We hope that this observation will motivate a continuing search of suitable frustrated magnetic materials for adiabatic demagnetization refrigeration applications.

[1] M. Zhitomirsky, Phys. Rev. B 67, 104421 (2003).

[2] P. Wikus et al., Cryogenics 62, 150 (2014).

[3] D.A. Paixao Brasileiro et al., Cryogenics 105, 103002 (2020).

[4] E. Lhotel et al., arXiv:2105:09817v1.

## (De)stabilization of non-ionic foam with ions

**J. Lamolinarie<sup>1</sup>**, L. Chiappisi<sup>1</sup>, O. Diat<sup>2</sup>, G. Fragneto<sup>1</sup>, L. Girard<sup>2</sup>, C. Pasquier<sup>2</sup>, P. Bauduin<sup>2</sup>, P. Lechevalier<sup>3</sup>, and J-L. Bridot<sup>3</sup>

<sup>1</sup> Institut Max von Laue-Paul Langevin, 71 avenue des Martyrs, 38042 Grenoble Cedex 9, France

<sup>2</sup> Institut de Chimie Séparative de Marcoule, ICSM, CEA, CNRS, ENSCM, Univ Montpellier, Marcoule, France

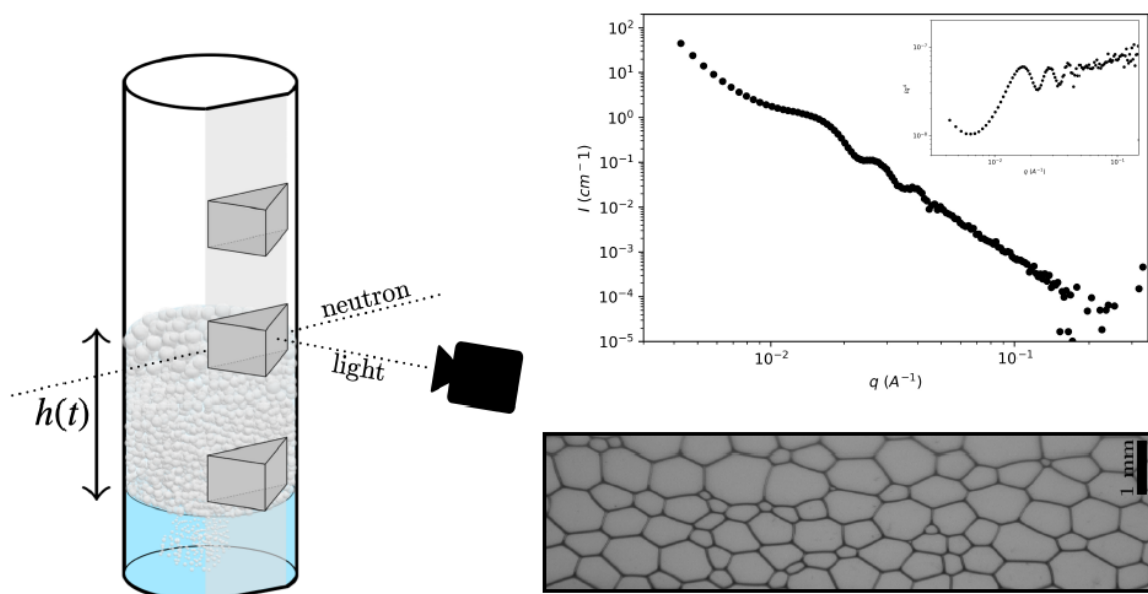
<sup>3</sup> Teclis Scientific, 22 Chemin des Prés Secs, 69380 Civrieux-d'Azergues, France

Very recently, it was shown that non-ionic foam aging could be strongly impacted by adding nanometersized anions (also called nano-ion) [1]. Indeed, when the charge density of a nano-ion is lower than  $12 \text{ e/nm}^3$ , these nano-ions have a superchaotropic behavior, i.e. that they can adsorb onto a polar and hydrated surface [2,3]. So, when superchaotropic nano-ions are solubilized within a foam made with a non ionic surfactant such as a polyethoxylated amphiphile, the nano-ions adsorb onto the surface and charge the interface that becomes repulsive. This repulsive interaction has been already observed and analyzed for micelles but not in real foam [3].

In this work, the first objective was to build a new cell in order to make a foam that can be studied simultaneously via small angle neutron scattering and macroscopic imaging (see Figure 1). Both measurements allow to correlate bubble size distribution and evolution with the bubble film thickness during the drainage and as a function of the height of the foam. The studied system was composed of BrijO10 in  $\text{D}_2\text{O}$  and the silicatungstic acid polyoxometallate as the nano-ion at different molar ratio. Comparisons were carried out using sodium dodecyl sulfate surfactant for which numerous studies were already published [4,5].

Figure 2 presents a typical scattering curve from a foam during the first step of the drainage. A  $Iq^4$  vs  $q$  plotted in the inset emphasize the oscillation coming from the reflected beam on the bubble interfaces. Figure 3 correspond to a picture of the foam structure at the same time.

From these mesoscopic and macroscopic information we expect to get deeper knowledge of all the mechanisms that are destabilizing the foam (foam drainage, bubble coarsening and coalescence).



[1] M. Hohenschutz, PhD : Nano-ions in interaction with non-ionic surfactant self-assemblies (article submitted, under review)

[2] T. Buchecker, et al, Chem. Commun., 2018, 54, 1833-1836

[3] M. Hohenschutz, et al, Angewandte International Edition, 59, 21 (2020), 8084-8088

[4] M. Axelons, et al, Langmuir, 2003, 19, 6598-6604

[5] E. Terriac, et al, Colloids and Surfaces A: Physicochem. Eng. Aspects 309 (2007) 112-116

# Surface magnons and crystalline electric field shifts at the nanoscale in superantiferromagnetic NdCu<sub>2</sub>

E. M. Jefremovas<sup>1</sup>, M. de la Fuente Rodríguez<sup>1</sup>, F. Damay<sup>2</sup>, B. Fak<sup>3</sup>, A. Michels<sup>4</sup>, J. A. Blanco<sup>5</sup> and L. F. Barquín<sup>1</sup>

<sup>1</sup> Dpto. CITIMAC, Facultad de Ciencias, Universidad de Cantabria, 39005 Santander, Spain.

<sup>2</sup> Laboratoire Léon Brillouin, CEA-CNRS, 91191 Gif-sur-Yvette Cedex, France.

<sup>3</sup> Institut Laue-Langevin, 38042 Grenoble, France

<sup>4</sup> Department of Physics and Material Science, University of Luxembourg, L-1511, Luxembourg. <sup>5</sup> Department of Physics, Universidad de Oviedo, 33007 Oviedo, Spain

In recent years we have been focused on the understanding of magnetism in ensembles of 4f metallic nanoparticles ( $R = \text{Tb, Nd, Gd}$ - $M = \text{Cu, Al, Y, La}$ ). As a result, we have reported that the existence of an ordered magnetic core and a disordered magnetic shell is regularly found in those ensembles. Depending on the stoichiometry (in our case  $\text{RX}_2$ ) it is possible to easily tune the RKKY interactions to provoke the appearance of ferromagnetic or antiferromagnetic order within the nanoparticles. The fact that we are dealing only with thousand of moments per particle leads to the use of the super- prefix to define correctly the behaviour [1].

A very upsetting fact is that both the collective moment dynamics and the role of the crystalline electric field at the nanoscale have barely been unearthed, in particular, in ensembles of nanoparticles. Thanks to our previous know-how we have come across the production of very large quantities of NdCu<sub>2</sub> nanoalloys. This is achieved by ball milling which is *the only route (top-bottom) to perform a profound analysis of those collective excitations via inelastic neutron scattering*. We are reporting here those results.

In our NdCu<sub>2</sub> nanoparticles, neutron diffraction measurements (LLB) indicate a mean nanoparticle size of  $\langle D \rangle \approx 13$  nm, where the bulk commensurate antiferromagnetic structure is retained at the nanoparticle core. Magnetic measurements evidence the interactions among the magnetic moments located at the nanoparticle surface which are strong enough to establish a Spin Glass behaviour. A Superantiferromagnetic state is therefore set for the NdCu<sub>2</sub> nanoparticles. Specific heat analyses show a broad Schottky contribution, with a maximum located at  $T \sim 25$  K, revealing the existence of crystalline electric field. Inelastic neutron scattering (ILL) analyses performed at  $T = 10$  K (paramagnetic state) and  $T = 1.5$  K (magnetic state) reveal the presence of both crystalline electric field and magnon collective excitations. Therefore, the splitting of the crystalline electric field levels associated with the Nd<sub>3+</sub> ions, as well as the spin-wave excitations that emerged below the Néel transition ( $T_N \approx 6$  K) in polycrystalline NdCu<sub>2</sub> [2] are maintained in the nanoparticle state. Additionally, we have been able to isolate the scattering contribution arising from the nanoparticle revealing that finite-size effects and microstrain lead to a partial inhibition of the transitions from the ground state to the first excited level, as well as a stiffening of the magnon modes [3].

[1] E. M. Jefremovas et al., *Nanomaterials* 10(2020), 6; E. M. Jefremovas et al., *Nanomaterials* 10 (2020) (11); C. Echevarría-Bonet et al. *PRB* 87 (2013) 18.

[2] E. Gratz et al. *J. Phys: Condens. Matter* 3 (1991), 9297

[3] E. M. Jefremovas et al., (submitted to *Phys. Rev. B*, 2021).

## SANS studies of polyelectrolyte in organic media

**Anish Gulati**<sup>1</sup>, Carlos G Lopez<sup>1</sup>, Ralf Schweins<sup>2</sup>, Olga Matsarskaia<sup>2</sup>, Takaichi Watanabe<sup>3</sup> and Walter Richtering<sup>1</sup>

<sup>1</sup> Institute of Physical Chemistry, RWTH Aachen University, Germany

<sup>2</sup> Institut Laue-Langevin, 71 Avenue des Martyrs, F-38042 Grenoble Cedex 9, France

<sup>3</sup> Department of Applied Chemistry, Graduate School of Natural Science and Technology, Okayama University, 3-1-1, Tsushima-naka, Kita-ku, Okayama, 700-8530, Japan

With the field of polyelectrolytes gaining importance in the recent years, there have increasing efforts to understand their behaviour under the influence of a range of internal and external factors. This is to aid the realization of their potential by grasping their applicability to various industrial and biological processes. In the initial part of this study, we look at the carboxymethyl cellulose CMC system. The Na salt of CMC is widely used as viscosity modifier. However, its utilization is limited as it is insoluble in organic solvents. We managed to overcome this by replacing the Na counterion with the Tetrabutylammonium (TBA) counterion, which lends it solubility in a wide array of solvents. Combining SANS and rheology we were able to explore the various properties of the CMC systems such as the correlation length ( $\xi$ ), overlap concentration ( $c^*$ ), entanglement concentration ( $c_e$ ), intrinsic viscosity etc. under the influence of the solvent parameters, for instance, the dielectric constant ( $\epsilon$ ). The SANS data were further evaluated alongside the rheological measurements for these systems, which resulted in some interesting observations. For instance, we observe a much weaker correlation from rheology measurements between overlap concentration ( $c^*$ ) and  $\epsilon$  than what we expect to see using the scaling laws. A similar observation is made for the correlation between specific viscosity ( $\eta_{sp}$ ) and  $\epsilon$ .

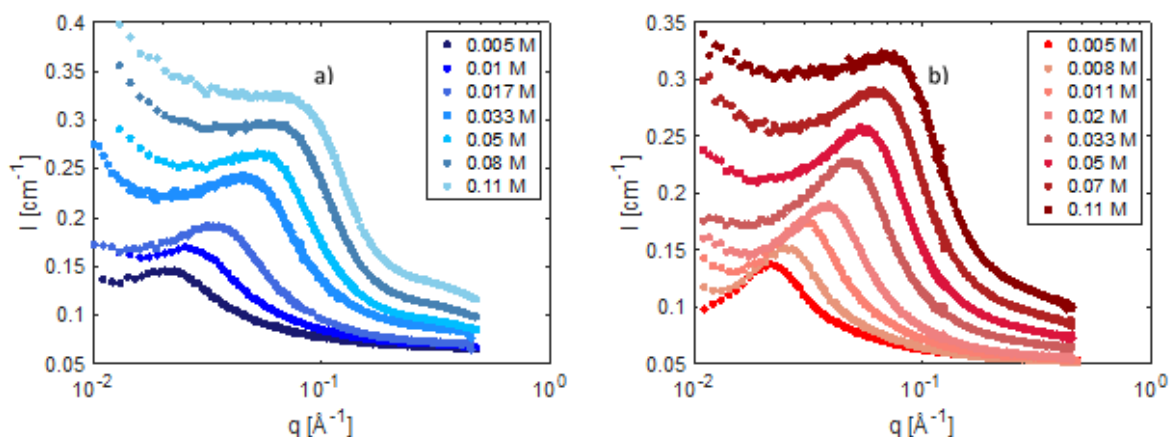


**Figure 1. SANS data for TBACMC in a) d-Methanol and b) d-DMSO**

Furthermore, so as to enhance our understanding of these systems, we are conducting a SANS study for polystyrene sulfonate (PSS) and a polyionic liquid ([Evim][Tf2N]). The NaPSS in water system has been extensively studied and this provides us with a reference to assess our system where we use to TBAPSS, which is again soluble in numerous solvents. Both TBAPSS and TBACMC show similar solubility to a large extent e.g., they are both soluble in alcohols and glycols. However, TBAPSS is, additionally, soluble in solvents such as isopropanol (secondary alcohol) and acetone (ketone) whereas TBACMC is insoluble in both of these. This allows us to look at a greater range of solvents. Conversely, [Evim][Tf2N] shows quite different tendencies as it is soluble in organic solvents with a low but insoluble in alcohols and water, which have a relatively higher  $\epsilon$ . Therefore, it is more complementary to TBAPSS and TBACMC by virtue of its solubility patterns.

# Field-space anisotropy in the magnetic phase diagrams and multipolar excitations of $\text{Ce}_{1-x}\text{La}_x\text{B}_6$ measured in a rotating magnetic field

D. S. Inosov,<sup>1</sup> S. Avdoshenko,<sup>2</sup> P. Y. Portnichenko<sup>1</sup>

<sup>1</sup>*Institut für Festkörper- und Materialphysik, Technische Universität Dresden, Häckelstraße 3, 01069 Dresden, Germany*

<sup>2</sup>*Leibniz-Institut für Festkörper- und Werkstoffforschung (IFW) Dresden, Helmholtzstraße 20, 01069 Dresden, Germany*

Cubic  $f$ -electron compounds commonly exhibit highly anisotropic magnetic phase diagrams consisting of multiple long-range ordered phases. Field-driven metamagnetic transitions between them may depend not only on the magnitude, but also on the direction of the applied magnetic field. Examples of such behavior are plentiful among rare-earth borides, such as  $\text{RB}_6$  or  $\text{RB}_{12}$  ( $R$  = rare earth). In our recent work [1], we used torque magnetometry to measure anisotropic field-angular phase diagrams of La-doped cerium hexaborides,  $\text{Ce}_{1-x}\text{La}_x\text{B}_6$  ( $x = 0, 0.18, 0.28, 0.5$ ). One expects that field-directional anisotropy of phase transitions must be impossible to understand without knowing the magnetic structures of the corresponding competing phases and being able to evaluate their precise thermodynamic energy balance. However, this task is usually beyond the reach of available theoretical approaches, because the ordered phases can be noncollinear, possess large magnetic unit cells, involve higher-order multipoles of  $4f$  ions rather than simple dipoles, or just lack sufficient microscopic characterization. Here we demonstrate that the anisotropy under field rotation can be qualitatively understood on a much more basic level of theory, just by considering the crystal-electric-field scheme of a pair of rare-earth ions in the lattice, coupled by a single nearest-neighbor exchange interaction. Transitions between different crystal-field ground states, calculated using this minimal model for the parent compound  $\text{CeB}_6$ , possess field-directional anisotropy that strikingly resembles the experimental phase diagrams. This implies that the anisotropy of phase transitions is of local origin and is easier to describe than the ordered phases themselves.

The field-directional anisotropy is also pronounced in the excitation spectrum of  $\text{CeB}_6$ , which we have investigated using inelastic neutron (INS) scattering combined with theoretical calculations done within a localized approach using the pseudospin representation for the  $\Gamma_8$  states [2]. Our work demonstrates that the rotating-field technique at fixed momentum can complement conventional INS measurements of the dispersion at a constant field and holds great promise for identifying the symmetry of multipolar order parameters and the details of intermultipolar interactions that stabilize hidden-order phases in rare-earth compounds.

[1] D. S. Inosov, S. Avdoshenko, P. Y. Portnichenko, E. S. Choi, A. Schneidewind, J.-M. Mignot, M. Nikolo, *Phys. Rev. B* **103** (2021), 214415.

[2] P. Y. Portnichenko, A. Akbari, S. E. Nikitin, A. S. Cameron, A. V. Dukhnenko, V. B. Filipov, N. Yu. Shitsevalova, P. Čermák, I. Radelytskyi, A. Schneidewind, J. Ollivier, A. Podlesnyak, Z. Huesges, J. Xu, A. Ivanov, Y. Sidis, S. Petit, J.-M. Mignot, P. Thalmeier, D. S. Inosov, *Phys. Rev. X* **10** (2020), 021010.

# Surface Pressure-Induced Interdiffused Structure Evidenced by Neutron Reflectometry in Cellulose Acetate/Polybutadiene Langmuir Films

Anne-Sophie Vaillard<sup>1</sup>, *Alae El Haitami*<sup>1</sup>, Philippe Fontaine<sup>2</sup>, Fabrice Cousin<sup>3</sup>, Philipp Gutfreund<sup>4</sup>, Michel Goldmann<sup>2,5,6</sup>, and Sophie Cantin<sup>1</sup>

<sup>1</sup> CY Cergy Paris Université, F95000, Cergy, France

<sup>2</sup> Synchrotron SOLEIL, L'Orme des Merisiers, 91192 Gif sur Yvette Cedex, France

<sup>3</sup> Laboratoire Léon Brillouin, Université Paris-Saclay, F-91191 Gif-sur-Yvette, France

<sup>4</sup> Institut Laue-Langevin, 38000 Grenoble, France

<sup>5</sup> Institut des NanoSciences de Paris, Sorbonne Université, 75252 Paris Cedex 05, France

<sup>6</sup> Faculté des Sciences Fondamentales et Biomédicales, Université de Paris, 75006 Paris, France

Binary blends of water-insoluble polymers are a versatile strategy to obtain nanostructured films at the air–water interface. However, there are few reported structural studies of such systems in the literature. Depending on the compatibility of the polymers and the role of the air–water interface, one can expect various morphologies. In that context, we probed Langmuir monolayers of cellulose acetate (CA), of deuterated polybutadiene (PBd) and three mixtures of CA/PBd at various concentrations by coupling surface pressure– area isotherms, Brewster angle microscopy (BAM), and neutron reflectometry at the air–water interface to determine their thermodynamic and structural properties. The homogeneity of the films in the vertical direction, averaged laterally over the spatial coherence length of the neutron beam ( $\sim 5 \mu\text{m}$ ), was assessed by neutron reflectometry measurements using  $\text{D}_2\text{O}/\text{H}_2\text{O}$  subphases contrast-matched to the mixed films. At  $5 \text{ mN/m}$ , the whole mixed films can be described by a single slightly hydrated thin layer. However, at  $15 \text{ mN/m}$ , the fit of the reflectivity curves requires a two-layer model consisting of a CA/PBd blend layer in contact with the water, interdiffused with a PBd layer at the interface with air (Figure 1). At intermediate surface pressure ( $10 \text{ mN/m}$ ), the determined structure was between those obtained at  $5$  and  $15 \text{ mN/m}$  depending on film composition [1]. This PBd enrichment at the air–film interface at high surface pressure, which leads to the PBd depletion in the blend monolayer at the water surface, is attributed to the hydrophobic character of this polymer compared with the predominantly hydrophilic CA.

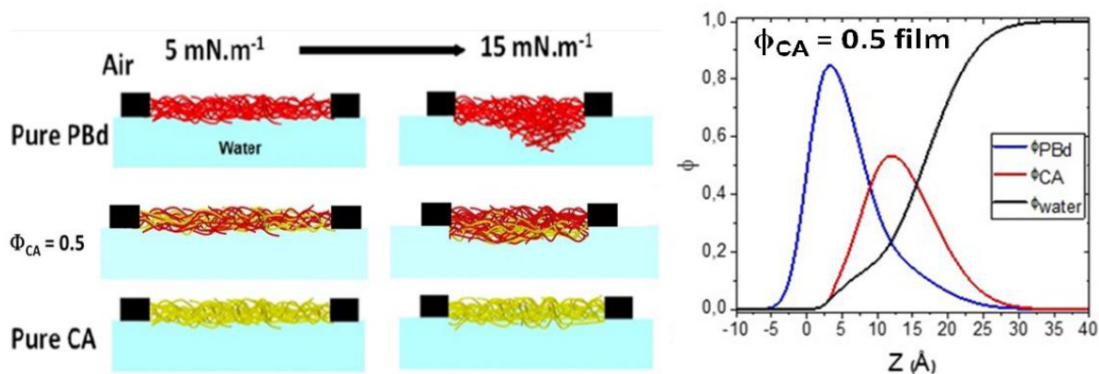


**Figure 1. Left. Schemes of the vertical structure determined by in situ neutron reflectivity of PBd, CA/PBd at a CA volume fraction  $\phi_{\text{CA}} = 0.5$  and CA Langmuir films at  $5$  and  $15 \text{ mN/m}$ , structures shown: red and yellow polymer chains correspond to PBd and CA, respectively. Right. CA, PBd and water volume fraction-depth profiles for  $\phi_{\text{CA}} = 0.5$  mixed film at  $15 \text{ mN/m}$ , deduced from the SLD-depth profiles using a two-layer model.**

[1] Anne-Sophie Vaillard, Alae El Haitami, Philippe Fontaine, Fabrice Cousin, Philipp Gutfreund, Michel Goldmann, Sophie Cantin, Langmuir, 2021, 37, 18, 5717–5730.

# On the use of statistical choppers to increase the performances of diffraction instruments on HiCANS

*F. Ott*<sup>1</sup>

<sup>1</sup> *Université Paris-Saclay, CEA-CNRS, Laboratoire Léon Brillouin, FRANCE*

Several institutes in Europe are considering the construction of new neutron sources using High-Current Low Energy Accelerator-based systems (HiCANS). We can mention the project SONATE in France, HBS in Germany or ARGITU in Spain. These new sources do not aim at competing with high-end sources such as ESS or the ILL but at providing flexible instrumentation to users for materials science studies. ESS as a long pulse source will be building very long instruments (up to 150m) to be able to achieve high resolution. On a HiCANS operating in long pulses mode, the performances would be limited for high resolution experiments.

We propose to revisit the use of statistical or Fourier choppers to implement them on a long pulse source so as to be able to build reasonably short and compact diffraction instruments on a CANS. Such choppers are for example used at Dubna (HRPD instrument) or SNS (CORELLI instrument).

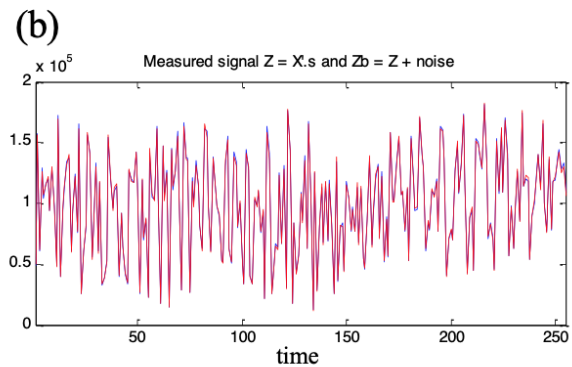
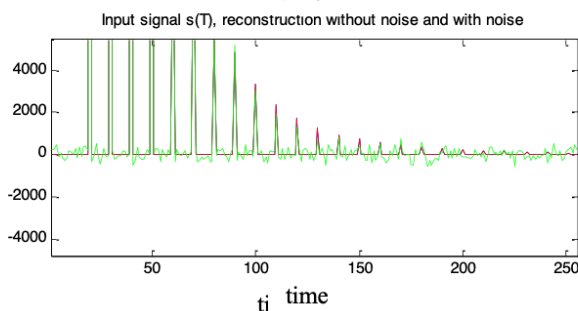
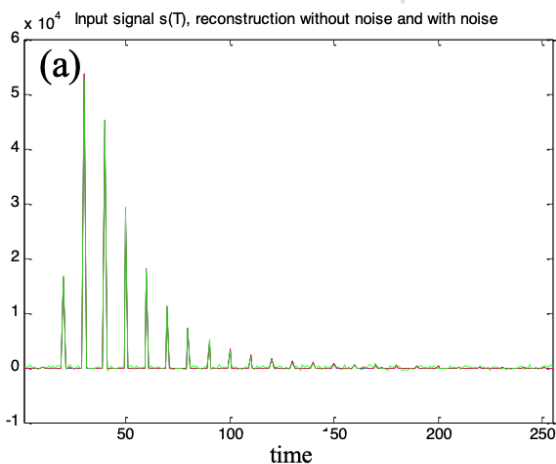
Statistical choppers allow either to increase the flux for a given resolution or increase the resolution for a given flight path.



*(Left) The CORELLI@SNS statistical chopper*

*(Bottom)*

- (a) Input signal  $s(t)$  with a ratio of 60 between the main pic and the lower intensity peak (red). (green) Reconstructed signal*
- (b) Time modulated measured signal. A 3% statistical noise has been added on the perfect signal.*
- (c) Ratio of the input signal and the reconstructed signal. Even on the lower intensity peaks (factor 60 wrt main peak), the intensity fluctuations are within 10%. The peaks position are perfectly defined though. This is suitable for following phase changes.*



## LLB CRG Inelastic instruments at ILL: from IN6 to Sharp, then Sharp+

**J.-M. Zanotti** <sup>1</sup>, S. Rodrigues<sup>1</sup>, P. Lavie<sup>1</sup>, B. Homatter<sup>1</sup>, S. Petit<sup>1</sup>, Q. Berrod<sup>2</sup>, P. Permingeat<sup>1</sup>, T. Robillard<sup>1</sup>, and F. Legendre<sup>1</sup>  
<sup>1</sup> Laboratoire Léon Brillouin (CEA-CNRS), Univ. Paris-Saclay, CEA Saclay, 91191 Gif-sur-Yvette, France  
<sup>2</sup> Univ. Grenoble Alpes, CNRS, CEA, IRIG-SyMMES, 38000 Grenoble, France

Following the agreement to strengthen the Franco-Swedish cooperation in the field of neutron scattering, the Laboratoire Léon Brillouin (LLB) has undertaken the construction of an inelastic time-of-flight spectrometer. After the announcement of the Orphée reactor shutdown in 2019, the project originally planned at Saclay could be transferred to the Laue Langevin Institute (ILL). This renaissance took the form of an A type CRG contract concluded on September 29<sup>th</sup> 2017 between the CEA DRF, the CNRS INP, and the ILL.

The SHARP (Spectromètre Hybride Alpes Région Parisienne) project has consisted in a complete rebuilding of the IN6 secondary spectrometer: sample environment, time-of-flight chamber and detection. SHARP takes advantage of 240 PSD (Position Sensitive Detector) detectors under 5 bars of <sup>3</sup>He. Beyond the gain of a factor 4 in detection coverage solid angle, these new detectors will allow a spectacular gain in the definition and mapping of the ( $Q$ ,  $\omega$ ) domains. This feature is a critical aspect to reach cutting edge capabilities in the field of single crystals-based physics. A major improvement concerns the time-of-flight chamber itself. It is now under vacuum (10<sup>-3</sup> mbar). A removable window between the sample and the inlet of the chamber enables to operate either with a sample under vacuum or under a controlled atmosphere. The number of windows between the sample and the detector has been minimized and offer a very positive gain in background. The second configuration makes it possible the study of samples to be kept under controlled atmosphere or in complex environment (laser or electrical excitation for example). The process of the Sharp construction has started right after the end of the 2020 last cycle (October) and was completed on March 21 2021 when the first neutrons have enlightened the brand-new instrument. This is a remarkable short time. A key part of the work has been the full refurbishing of the chamber with Cd coverage, installation of 240 PSD detectors along with their collimators and the associated electronics. As for the detections electronics, ILL technical teams have joined the LLB work-force for their cabling, testing and integration within the Data Acquisition System. Also, a very efficient pumping system has been designed and installed by the ILL vacuum group. After a cycle of commissioning, the instrument now welcomes users granted official beam time (50% 2FDN, 50% ILL).

**The future of SHARP:** Two long ILL shutdowns are needed for reactor work and for the re-construction and extension the of the H15 guide. By the end of this processes, in April 2024, the secondary spectrometer of Sharp will be moved to the end of this new H15 guide. The instrument will then become Sharp+. Sharp+ will take advantage of a guide-end position. The instrument will combine two modes: a Time Focusing (TF) mode as on IN6 and an additive so-called Monochromatic Focusing (MF) mode. TF will primarily beneficiate to quasi-elastic studies in soft matter and experiments in solid state physics where a good resolution (few hundreds of eV) is needed on a narrow range of energy transfer on the neutron energy loss side. The MF mode is optimized for studies requiring an almost constant resolution on a wide range of energy transfer (mainly studies in the field of material science). The switch from the MF to the TF mode will be possible by retracting a 4.5 meter-long section at the end of a 14 meter vertically and horizontally elliptic converging guide section (turn-key system *i.e.* no manpower required).

The instrument will be equipped by a  $Width*Height=20*30$  cm<sup>2</sup> two faces horizontal and vertical focusing monochromator. On one side, Pyrolytic Graphite will be used for incident wavelengths from 2 to 6 Å. On the other side Fluorinated Mica for wavelengths from 7 to 12 Å is foreseen (project under development). To be able to use incident wavelength from 2 to 4 Å, the instrument will not be equipped with a beryllium filter (BF). This will avoid a 15-20% absorption of the beam scattered by the monochromator and will reduce the health physics protection of the instrument. Instead of using a BF, the suppression of harmonics of the nominal wavelength will be ensured by 3 disk choppers cascade installed in the guide downstream of the monochromator. The counting rate of Sharp+ will be at least one order of magnitude larger than the one of IN6 (according to McStas simulations, a factor 15 is expected) and with a significantly reduced background.

# Autonomous Experiments in Inelastic Neutron Scattering

**M. Boehm**<sup>1</sup>, M. Noack<sup>2</sup>, T. Weber<sup>1</sup>, Y. LeGoc<sup>1</sup>, J. Sethian and P. Mutti<sup>1</sup>

<sup>1</sup> Institut Laue-Langevin, 71 avenue des Martyrs, CS 20156, 38042 Grenoble Cedex 9, France

<sup>2</sup> The Center for Advanced Mathematics for Energy Research Applications CAMERA, Lawrence Berkeley National Laboratory, Berkeley, CA 94720, United States of America

Autonomous experiments rely on modern machine learning algorithms for steering experimental data acquisition in a multidimensional parameter space without human intervention. Autonomous data acquisition becomes increasingly important for the execution and analysis of ever more complex experiments in many different scientific and industrial domains [1]. In autonomous learning, algorithms learn from a comparably little amount of input data and decide themselves on the next steps to take in a closed loop.

One promising direction for an efficient algorithm that is currently explored is the use of Gaussian Process Regression (GPR) [2]. GPR provides a quick non-parametric and robust approximation and uncertainty quantification method. In the context of autonomous experiments it can be used to estimate the posterior mean and covariance and uses them in a function optimization to calculate the optimal next measurement point. The posterior is based on a prior Gaussian probability density function, which is repeatedly retrained on previously measured points.

For the first time on a neutron spectrometer we used the GPR based algorithm gpCAM [3-5], developed by the CAMERA team at LNBL, in order to test the potential of this method for the typical point-by-point data acquisition of a classical three-axis spectrometer. In several test experiments gpCAM took control over the measurement process, without the intervention of the instrument scientists. Completely ‘agnostic’, i.e. without any prior information on the physical model or expected signal of the measured sample, the algorithm explored various accessible regions in the sample’s reciprocal space and reconstructed the signal with a strongly reduced number of total measuring points compared to a conventional ‘grid’ scanning technique (i.e. const-Q, const-E scans).

In this talk we will introduce this new experimental procedure and compare it to traditional data acquisition on three-axis spectrometers. We try to show a perspective of the future experimental possibilities and how the scientific measurements could evolve in conjunction with modern algorithms.

[1] Noack, M.M., Zwart, P.H., Ushizima, D.M. *et al.* Gaussian processes for autonomous data acquisition at large-scale synchrotron and neutron facilities. *Nat Rev Phys* (2021). <https://doi.org/10.1038/s42254-021-00345-y>.

[2] for an introduction, see e.g. C. E. Rasmussen and C. K. I. Williams, *Gaussian Processes for Machine Learning*, the MIT Press, 2006, ISBN 026218253X. © 2006 Massachusetts Institute of Technology. [www.GaussianProcess.org/gpml](http://www.GaussianProcess.org/gpml).

[3] <https://gpcam.lbl.gov>.

[4] Marcus Noack and Petrus Zwart. Computational strategies to increase efficiency of gaussian- process-driven autonomous experiments. In *2019 IEEE/ACM 1st Annual Workshop on Large-scale Experiment-in-the-Loop Computing (XLOOP)*, pages 1–7. IEEE, 2019.

[5] Marcus M Noack, Kevin G Yager, Masafumi Fukuto, Gregory S Doerk, Ruipeng Li, and James A Sethian. A kriging-based approach to autonomous experimentation with applications to x-ray scatter- ing. *Scientific Reports*, 9:11809, 2019.

## **NeXT-Grenoble, the Neutron and X-ray Tomograph at ILL**

Alessandro Tengattini<sup>1</sup>, Lukas Helfen, Cyrille Couture, Nicolas Lenoir, Cino Viggiani

<sup>1</sup> *Institut Laue-Langevin, 71 avenue des Martyrs, CS 20156, 38042 Grenoble Cedex 9, France*

Neutron imaging is a powerful non-destructive method for probing matter in 3D, capable of tackling questions from a plethora of scientific areas. A range of advanced imaging techniques are also rapidly developing and expanding the range of available contrast options, such as phase contrast, and polarised neutron imaging. Due to its non-destructive nature, it is possible to acquire multiple 3D volumes as the sample evolves, for example through chemo-thermo-hydro-mechanical loading, which in turn allows the spatio-temporally resolved quantification of processes. Recent technological developments even allow the simultaneous acquisition of highly complementary x-ray tomographies.

This presentation will review the fundamental elements of neutron imaging, from the fundamental equations governing it, to the neutron production and detection. It will also attempt to provide an overview of the advanced techniques developed in recent years and provide an outlook of ongoing and future developments.